Topographic Heterogeneity and Aspect Moderate Exposure to Climate Change Across an Alpine Tundra Hillslope

Katya R Jay[1], K R Jay[2,3,4], W R Wieder[2,5], S C Swenson[5], J F Knowles[3], S Elmendorf[2,4], H Holland-5 Moritz[6], K N Suding[2,4,6], and Katya Jay[1]

[1]Affiliation not available
[2]Institute of Arctic and Alpine Research, University of Colorado
[3]Department of Earth and Environmental Sciences, California State University
[4]Department of Ecology and Evolutionary Biology, University of Colorado
[5]National Center for Atmospheric Research
[6]Department of Natural Resources and the Environment, University of New Hampshire

July 27, 2023

Topographic Heterogeneity and Aspect Moderate Exposure to Climate Change Across an Alpine Tundra Hillslope

K. R. Jay[1], W. R. Wieder[1,2], S. C. Swenson[2], J. F. Knowles[3], S. Elmendorf[1,4], H. Holland-Moritz[5], K. N. Suding[1,4]

[1]Institute of Arctic and Alpine Research, University of Colorado, 4001 Discovery Dr, Boulder, CO 80303, USA.

[2]National Center for Atmospheric Research, 1850 Table Mesa Dr, Boulder, CO 80305, USA

[3]Department of Earth and Environmental Sciences, California State University, 400 W. First St, Chico, CA 95929, USA.

[4]Department of Ecology and Evolutionary Biology, University of Colorado, 1900 Pleasant St, Boulder, CO 80302, USA.

[5]Department of Natural Resources and the Environment, University of New Hampshire, 114 James Hall, 56 College Rd, Durham, NH 03824, USA.

Corresponding author: Katya Jay (katya.jay@colorado.edu)

Key Points:

- Local abiotic heterogeneity (via differences in topography and aspect) governs snow accumulation, runoff, and productivity in alpine tundra
- Climate warming leads to earlier snowmelt, decreased runoff, and drier soils, potentially decoupling plant resource demand and availability
- Topographic position mediates exposure to climate change, highlighting potential vulnerabilities of moisture-limited vegetation patches

Abstract

Alpine tundra ecosystems are highly vulnerable to climate warming but are governed by local-scale abiotic heterogeneity, which makes it difficult to predict tundra responses to environmental change. Although land models are typically implemented at global scales, they can be applied at local scales to address process-based ecological questions. In this study, we ran ecosystem-scale Community Land Model (CLM) simulations with a novel hillslope hydrology configuration to represent topographically heterogeneous alpine tundra vegetation across a moisture gradient at Niwot Ridge, Colorado, USA. We used local observations to evaluate our simulations and investigated the role of topography and aspect in mediating patterns of snow, productivity, soil moisture, and soil temperature, as well as the potential exposure to climate change across an alpine tundra hillslope. Overall, our simulations captured observed gradients in abiotic conditions and productivity among heterogeneous, hydrologically connected vegetation communities (moist, wet, and dry). We found that south facing aspects were characterized by reduced snowpack and drier and warmer soils in all communities. When we extended our simulations to the year 2100, we found that earlier snowmelt altered the timing of runoff, with cascading effects on soil moisture, productivity, and growing season length. However, these effects were not distributed equally across the tundra, highlighting potential vulnerabilities of alpine vegetation in dry, wind-scoured, and south facing areas. Overall, our results demonstrate how land model outputs can be applied to advance process-based understanding of climate change impacts on ecosystem function.

Plain Language Summary

It is critical to understand how rapidly warming mountain ecosystems will respond to environmental change. However, large differences in physical properties, including temperature,

snow, and water, over small distances make it difficult to project these responses. We used a land surface model that captures distributions of water and energy across the landscape paired with long-term observations from an alpine ecosystem to explore changes in snow, water, and productivity among diverse alpine vegetation. Additionally, we explored how this ecosystem might respond to climate change and how these responses differ across north and south facing slopes. Overall, our model results matched patterns in physical conditions and plant productivity observed at this site. We found that south facing slopes had less snow and drier, warmer soils compared to north facing slopes. Responses to climate change included snow melting earlier in the year, shifting the timing of runoff and suggesting that plant water demand may become disconnected from resource availability. Furthermore, responses differed across the landscape, indicating that plants in dry, wind-scoured, and south facing areas are more vulnerable to environmental change. Our study examines local-scale variation across an alpine landscape to address the challenge of projecting responses to change in rapidly warming ecosystems.

1 Introduction

Alpine and arctic tundra ecosystems are particularly sensitive to climate variability and change (Ernakovich et al., 2014; Seddon et al., 2016). Global air temperatures are rising, and high-elevation regions are warming faster than the rest of the planet; alpine records show an average rate of 0.3°C ± 0.3 ˚C/decade compared to 0.2°C ± 0.1 ˚C/decade globally (Hock et al., 2019). Mountain regions provide critical ecosystem services including supplying drinking water to half of the global population, but these water supplies are highly sensitive to climate change (Immerzeel et al. 2020). Moreover, warming in these high-elevation systems has potential implications for global carbon cycling via accelerated permafrost degradation (Knowles et al.,

2019), as has been shown in high-latitude permafrost systems (Schuur et al., 2015). Additional impacts of increasing temperatures in alpine systems include decreased snowpack (Musselman et al., 2021; Wieder et al., 2022), altered nutrient cycling (Dong et al., 2019), shifts in the timing of the growing season, and changes in vegetation composition (Walker et al., 2006). The exposure to these projected changes, however, may not be experienced evenly over alpine ecosystems.

Topographic gradients (formed by lateral drainage from hills to valleys) and aspect-driven differences in solar radiation represent primary controls on the availability of water and energy across landscapes, and thus the distribution of soil water and vegetation within ecosystems (Fan et al., 2019; Swenson et al., 2019). In mountainous terrain, topographic complexity at micro- and macro-scales (tens to thousands of meters, here referred to as 'hillslope scales'; Swenson et al., 2019) drives variability in the accumulation and redistribution of snow and water – leading to gradients in soil conditions, hydrologic connectivity, nutrient cycling, and vegetation composition (Erickson et al., 2005; Opedal et al., 2015). Abiotic heterogeneity at hillslope scales can lead to microclimate differences where some parts of the landscape are buffered from atmospheric changes and act as refugia while other areas are more exposed, accentuating potential vulnerabilities (Lenoir et al., 2017; McLaughlin et al., 2017). Microscale variation can also mediate responses to climate warming (Körner & Hiltbrunner, 2021; Winkler et al., 2018; Zellweger et al., 2020), making it more difficult to predict how these systems will respond to change. Thus, exposure to climate change will likely be moderated by the heterogeneity generated by topographic complexity in mountain landscapes, where differences in topography and aspect alter abiotic conditions such as surface temperature, snow accumulation, and soil moisture. In the Colorado (CO) Rocky Mountains, slopes are predominantly north- and south-facing as a result of east-west draining valleys, leading to prominent variation in seasonal

snowpack depth and vegetation composition across aspects (Daubenmire, 1943; Helm, 1982; Hinckley et al., 2012). However, few studies have examined the role of topographic gradients and aspect in shaping patterns of snow, moisture, and productivity across alpine tundra landscapes and mediating their responses to climate warming.

At Niwot Ridge, CO, a Long-Term Ecological Research (LTER) site, a 70-year climate record shows that maximum annual temperatures have been increasing faster than the global rate at ~0.5 ˚C/decade (McGuire et al., 2012). Concurrent shifts in environmental conditions including precipitation and atmospheric deposition complicate efforts to understand alpine rates of response to warming. Indeed, previous studies have found conflicting responses that indicate alpine tundra ecosystems will both lag behind (Alexander et al., 2018; Körner & Hiltbrunner, 2021) and track (Panetta et al., 2018; Steinbauer et al., 2018) climate changes. Regional studies show that rising air temperatures have already led to earlier snowmelt and streamflow, as well as increases in the length of the ice-free period in alpine lakes (Christianson et al., 2021; Musselman et al., 2021). Heterogeneous terrain at Niwot Ridge leads to spatial variability in hydrologic connectivity, soil moisture, plant productivity, nitrogen (N) mineralization rates, and microbial biomass across the landscape (Chen et al., 2020; Hermes et al., 2020; Schmidt et al., 2015). Thus, we expect the effects of warming on nutrient cycling, productivity, and plant community composition to vary with topography and aspect.

To better understand how local heterogeneity mediates ecosystem responses to climate change, we used a land model with hillslope-scale processes to represent a heterogeneous alpine environment and examine ecological hypotheses. Land models simulate biophysical and biogeochemical processes, representing water, energy, carbon (C), and N fluxes (Lawrence et al., 2019). While these models are primarily used at global scales, they can be leveraged to address

ecologically relevant questions and provide insight into abiotic and biotic responses to climate change at regional and local scales (Mao et al., 2016). For example, Wieder et al. (2017) used the Community Land Model (CLM) version 4.5 to represent local patterns of water, energy, and C in alpine tundra, showing promise in exploring ecological responses to change. We build on this work using eddy covariance measurements from 2008-2021 at Niwot Ridge, CO to run single-point simulations of the CLM5 (Lawrence et al. 2019) with a hillslope hydrology configuration (Swenson et al. 2019) and site-specific modifications for moist, wet, and dry alpine vegetation (Figure 1). We first asked whether our modeling framework could reproduce observations of snow, soil temperature and moisture, and productivity across a topographically complex tundra hillslope *(Model evaluation)*. We then applied this framework to examine how differences in solar radiation across north and south aspects alter patterns of hydrology, soil moisture and temperature, and growing season length *(Model application)*. Finally, we extended our simulations to 2100 and examined whether microscale variation (via aspect and vegetation community) moderates exposure to climate change and ecosystem services *(Model projection)*.

2 Methods

2.1 Study site

Our study was conducted at Niwot Ridge, a high-alpine LTER site in the Front Range of the CO Rocky Mountains, USA (40˚03’ N, 105˚35’ W, altitude approximately 3500 m above sea level, asl). Niwot Ridge has a mean annual temperature of -2.2˚C and receives 884 mm of precipitation annually. Long term climate measurements from 1953–present at the D-1 site that hosts the highest elevation long-term weather station in North America at 3749 m asl show a strong warming trend at Niwot Ridge during the spring and summer months (Bueno de Mesquita

et al., 2021; McGuire et al., 2012). Precipitation patterns are highly variable and show a slight increase over time at alpine sites (Kittel et al., 2015). Indeed, high variability in total annual precipitation and mean monthly air temperatures seems characteristic of the site (Walker et al., 1994). Most of this precipitation (80%) falls as snow (Caine, 1996), leading to a short 2-3 month growing season. Niwot Ridge ecosystems range from subalpine forests to alpine tundra and talus. Our work here focuses on the dry, moist, and wet meadow vegetation that is broadly characteristic of alpine tundra ecosystems at the site.

Alpine tundra vegetation is structured largely by snow and its redistribution by wind across the topographically variable landscape (Erickson et al., 2005; Litaor et al., 2008), with some areas accumulating snow while other areas remain wind-scoured and snow free. Snow free areas, which host fellfield vegetation, and areas with thin snow cover, which host dry meadow vegetation, tend to be less productive and have low statured vegetation due to temperature and moisture adaptations (Billings & Mooney, 1968). In contrast, areas with deep snow accumulation host moist meadow communities, where snow persists into the summer and productivity is higher. Wet meadow vegetation forms in lowland areas that receive runoff from upland snowmelt and tend to have the highest productivity.

2.1.1 Site observations for model forcing and evaluation

Local meteorological measurements are necessary to run single-point CLM simulations. Most inputs were available from alpine stations at Niwot Ridge (Figure 1), but we leveraged measurements from nearby subalpine stations as necessary. Specifically, we used air temperature, relative humidity, barometric pressure, and wind speed inputs measured at two alpine eddy covariance towers, which are located in fellfield and dry meadow vegetation (3480

m asl, AmeriFlux sites US-NR3 and US-NR4; Knowles, 2022a, 2022b; Knowles et al., 2012). We used measurements from US-NR4 and gap-filled them using measurements from US-NR3 when necessary. Precipitation data came from the nearby Saddle site (3525 m asl) and were corrected for the effects of blowing snow from October–May following Williams et al. (1998). We used these data in combination with a half-hourly precipitation record from the subalpine U.S. Climate Reference Network (USCRN) station 14W (40˚02' N, 105˚32' W; data from https://www.ncei.noaa.gov/pub/data/uscrn/products/subhourly01/; accessed May 2022) measured at 3050 m asl to distribute the Saddle precipitation record to the half-hour measurements needed for CLM, following methods described in previous work (Wieder et al., 2017). Finally, incoming shortwave radiation data were taken from a lower elevation eddy covariance tower, also located in subalpine forest (Ameriflux site US-NR1, 3050 m asl; Burns et al., 2016), as incoming solar measurements from higher elevations sites were not reliably collected over the alpine data record (again, as in Wieder et al. 2017). Meteorological data were gap-filled using the R package REddyProc (Wutzler et al., 2018).

We evaluated model results by comparing them with ongoing, publicly available Niwot Ridge datasets, including snow depth collected ~biweekly from 88 gridded points since 1982 (Walker et al., 2022) and corresponding descriptions of dominant plant communities (Spasojevic et al., 2013). We also compared our results with biomass harvests collected at the end of the growing season to estimate annual aboveground net primary productivity (ANPP; Walker et al., 2022). These ANPP measurements were multiplied by 0.5 to convert g dry weight to g C for direct comparison with model outputs. For the dry meadow, we compared our simulations with gross primary productivity (GPP) estimates from the alpine flux towers (Knowles, 2022a, 2022b). Finally, we used soil moisture and temperature data collected since 2018 from the

Sensor Network Array at Niwot Ridge (Morse & Niwot Ridge LTER, 2022) to evaluate our simulations (Figure 1).

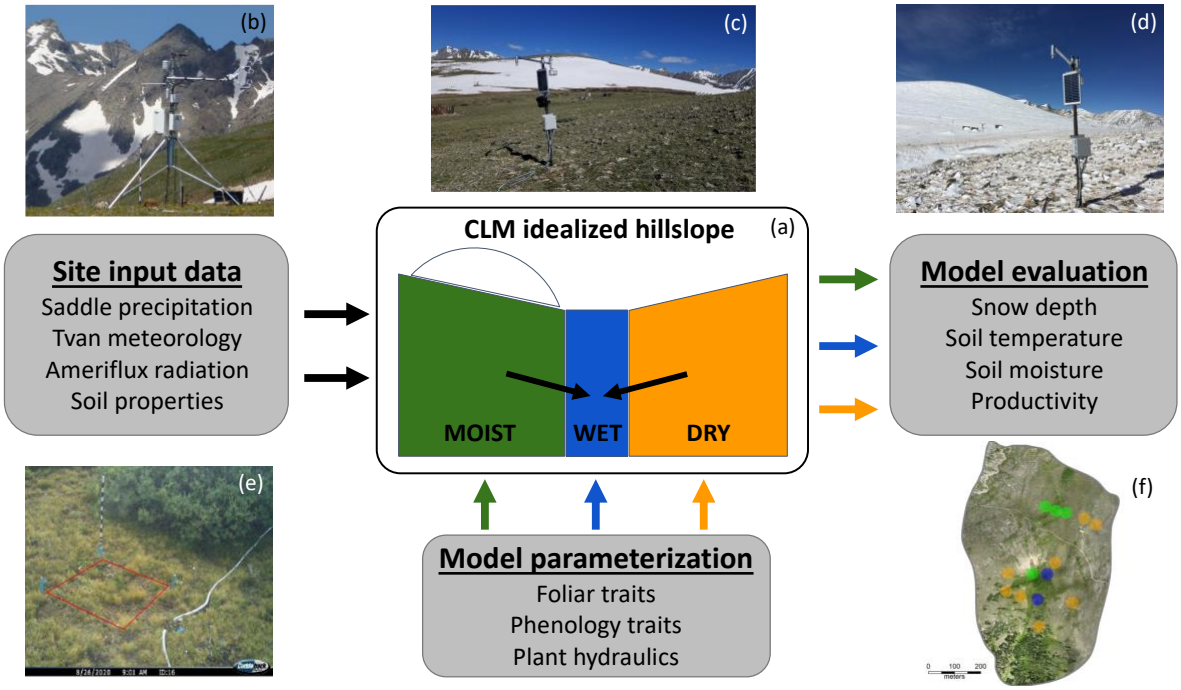

Figure 1. The Community Land Model (CLM) can be run at point scales and with site-specific configurations to test ecological hypotheses using a combination of atmospheric forcings, plant traits, and observational data for evaluation, as shown in this diagram of our model workflow for single-point simulations with hillslope hydrology configured for an alpine tundra hillslope. (a) shows the Niwot Ridge idealized hillslope, with separate columns for moist, wet, and dry meadow vegetation. Black arrows indicate the direction of hydrologic connectivity with a lowland (wet meadow) column connected to two upland (moist and dry meadow) columns. Forcing data included meteorological measurements from two alpine flux towers (b, photo credit J. Knowles), precipitation measurements from the Saddle site (c, photo credit W. Wieder; d, photo credit J. Morse), and shortwave radiation measurements from the US-NR1 AmeriFlux Tower site. Moist, wet, and dry meadows were parameterized using plant functional trait data and phenocam observations (e) from Niwot Ridge. We used observational data from Niwot Ridge including snow depth measurements, soil temperature and moisture from the Sensor Network Array (f, aerial imagery from Wigmore & Niwot Ridge LTER, 2021), and aboveground NPP measurements from biomass harvests to evaluate our results.

2.2 CLM overview

We ran single-point simulations of the CLM version 5 (Lawrence et al., 2019), the land component of the Community Earth Systems Model (CESM; Danabasoglu et al., 2020), with the hillslope hydrology configuration (Swenson et al., 2019) and active biogeochemistry, including

vertically resolved soil biogeochemistry (Koven et al., 2013) and site-level modifications to represent Niwot Ridge conditions. Our single-point CLM simulations approximate the footprint of an eddy covariance tower and allow ecological hypotheses to be tested and generated (Bonan et al., 2011; Hudiburg et al., 2013; Wieder et al., 2017). The hillslope hydrology configuration in CLM explicitly represents the effects of topography on insolation and the lateral redistribution of water at the scale of an average or 'representative' hillslope (Swenson et al., 2019).

For our representative hillslope at Niwot Ridge, we wanted to represent hydrological conditions at the well-studied Saddle site where topography and aspect control patterns of snow accumulation and vegetation distribution. To do this we implemented three hydrologically connected columns within the vegetated land unit, with one downslope 'lowland' column (wet meadow) and two upslope columns (moist and dry meadows; see Figure 1). In this configuration, surface and subsurface lateral flow was passed between neighboring columns and runoff from the lowland column was passed directly into the stream channel. See Swenson et al. (2019) for a detailed description of possible hillslope configurations and hillslope-scale hydrological processes in CLM. The number of columns within our hillslope and the connectivity between columns was prescribed by an input surface data set. The slope and aspect of each column was also prescribed by the surface data set, with the two upland columns having slopes of 0.3 m/m and east and west aspects (moist and dry meadow columns, respectively; Figure 1).

All simulations were spun up in "accelerated decomposition" mode for 200 years by cycling over four years of forcing data from 2008-2011; soil and vegetation C and N pools were then allowed to equilibrate for another 100 years (Lawrence et al., 2019). Historical simulations were conducted using observations of atmospheric data over the experimental period from 2008-2021. We ran historical simulations with fixed CO_2 concentrations.

232

233 2.2.1 Site-specific model setup

234 To better represent local conditions across vegetation communities in the Saddle, we
235 made several site-specific modifications related to meteorological input data, surface
236 characterizations, and parameterizations of the default Arctic C_3 grass plant functional type used
237 in the CLM. Strong winds redistribute snow across Niwot Ridge (Erickson et al., 2005), leading
238 to patchy distribution of snow that structures vegetation communities. Snow accumulates on
239 leeward (east facing) slopes that support productive moist meadow communities with grasses
240 (e.g., *Deschampsia caespitosa*) and forbs (e.g., *Acomastylis rossii*), whereas windward (west
241 facing) slopes have little snow accumulation and support characteristic dry meadow communities
242 dominated by sedges (e.g., *Kobresia myosuroides*). The physics of the CLM does not represent
243 this fine scale, sub-grid redistribution of snow by wind, so we directly modified winter
244 precipitation levels: when air temperatures were below 0°C, moist meadow columns, which
245 accumulate the deepest winter snowpack, received 100% of observed Saddle precipitation, wet
246 meadow columns received 75% of observed precipitation, and dry meadow columns received
247 only 10% of observed precipitation. When air temperatures were above freezing all columns
248 received identical precipitation (as rain). These modifications result in maximum snow depths
249 that align with periodic snow depth measurements for these landscape positions that are collected
250 across the Saddle grid and have been used in previous work at the site (Wieder et al., 2017).

251 Variations in soil properties across Niwot Ridge also reflect differences in snow
252 accumulation and vegetation communities, with wetter parts of the landscape having deeper,
253 more developed soils (Burns, 1980). Accordingly, we used National Ecological Observatory
254 Network (NEON) Megapit data (Lombardozzi et al., 2023) to modify soil properties that reflect

these differences in soil characteristics seen in the field (Table S1). Specifically, for the rocky and less developed soils found in the dry meadow, we reduced water saturation by 50%. We also modified organic matter values based on data from Niwot Ridge (Burns, 1980) by reducing the organic matter fraction by 25% in moist and dry meadows to reflect that wet meadow soils have higher organic matter content than moist and dry meadows, and reduced sand content and increased clay content by 10% in the wet meadow. Lastly, we decreased the thickness of the dry surface layer, which controls soil evaporation (Swenson & Lawrence, 2014), by 33%.

Alpine tundra supports high floristic diversity with clear differences in functional traits that influence rates of photosynthesis and productivity in CLM (Fisher & Koven, 2020; Spasojevic et al., 2013). Accordingly, we modified foliar traits and phenology based on observations to represent moist, wet, and dry meadow vegetation (see Table S1). For foliar traits, we used functional trait data collected at Niwot Ridge over the past three decades (Spasojevic et al., 2013). We changed specific leaf area and foliar C:N ratios using median values calculated for each of the three communities. We also modified fine root to leaf allocation for each community based on observations and values from the literature (Table S1; Birch et al., 2021; Fisk et al., 1998). For phenology parameters, we used green chromatic coordinate (GCC) values extracted from phenocam observations from 2018-2022 at plots throughout the Saddle (Elwood et al., 2022) and phenometrics calculated from GCC values (unpublished data) to modify the timing of the growing season for each community. Phenometrics included start of growing season (50% of maximum GCC) and peak of growing season (maximum GCC) dates. We used 5 cm soil temperature observations and start of growing season dates in each community to calculate accumulated growing degree days (GDD; when surface soil temperatures >0˚C) before the start of leaf onset. Using these calculations, we modified a GDD scale factor in the model to represent

the increased GDD accumulation required in the dry meadow to trigger leaf out (a 70% increase compared to moist and wet meadows). We also calculated the number of days between leaf onset and peak greenness for each community (modifying *ndays_on* in Table S1).

When preliminary simulations showed high productivity biases compared to observations for all three communities, we modified several photosynthetic and plant hydraulic parameters to better represent alpine growth strategies (see Table S1). We first decreased two parameters in the mechanistic model of photosynthetic capacity used in CLM5 (leaf utilization of N for assimilation or LUNA; Ali et al., 2016) for all communities. These two parameters, j_{maxb0} and j_{maxb1}, specify the baseline proportion of N allocated for electron transport and the response of electron transport rate to light availability, respectively. To represent more conservative growth strategies in dry meadow vegetation, we decreased two plant hydraulic stress parameters representing maximum stem and root conductivity (Kennedy et al., 2019).

2.3 Model application and projection

After validating our model results against observations, we conducted two experimental simulations to quantify potential (1) effects of aspect on solar radiation that may moderate timing and magnitude of snowpack accumulation and runoff with cascading influences on soil moisture, soil temperature, and productivity on north and south facing slopes; and (2) interacting effects of aspect and climate change-induced warming across moist, wet, and dry meadows.

First, we ran two additional simulations to examine effects of aspect with the model setup as described above with several modifications. These simulations replicated the setup of our control (Saddle) simulations, except that the slope and aspect were modified to represent either a north or a south facing hillslope. We maintained the same precipitation inputs, vegetation

community parameterizations, and slope angle across all communities for consistency between control, south, and north facing simulations.

Second, to simulate climate change effects, we used an anomaly forcing protocol (Wieder et al. 2015), which provides a smooth transition between the observed alpine eddy covariance tower record (2008-2021) and a projected SSP3-7.0 scenario simulated by CESM2. Specifically, mean monthly changes (or anomalies) in the atmospheric state were calculated by subtracting the climatological mean of a 'historic' baseline, 2005-2014, from CESM2 projections under the SSP3-7.0 scenario through the end of the century. We added the atmospheric anomalies for the gridcell containing Niwot Ridge to meteorological data from the alpine flux tower that was cycled over the observational record. In addition to the atmospheric anomalies, the projected climate change scenario also included transient atmospheric CO_2 concentrations reaching 867 ppm by 2100 based on projected increases in emissions following protocols from the most recent Coupled Model Intercomparison Project (CMIP6) using CESM2. These future scenarios were run for all three vegetation communities on north and south facing aspects. We note that because climate trajectories may be accelerated at higher elevations (Mountain Research Initiative EDW Working Group, 2015; Wang et al., 2016), this approach represents a conservative estimate for changes in the mean atmospheric state that may be expected under this high emissions scenario. We also acknowledge that our approach represents a single possible climate change trajectory, but this balanced approach offers generalizable insight into how exposure to climate change may vary with aspect across topographically complex terrain.

3 Results and Discussion

3.1 Model evaluation: Niwot Ridge LTER measurements

Overall, the ecosystem-level CLM simulations agreed with observed patterns of soil

moisture, temperature, and snow depth from Niwot Ridge. Redistribution of snow by wind leads to three distinct vegetation communities that differ in their annual cycles of soil temperature, soil moisture, and productivity (Table 1), described in more detail below. Consistent with observations, simulated moist meadow and wet meadow communities are buffered from seasonal temperature extremes and remain relatively moist throughout their short growing season, whereas dry meadow communities experience wider seasonal fluctuations in soil temperature with longer, drier growing seasons.

Table 1. Comparison of key metrics related to snow, water, productivity, and soil conditions between moist, wet, and dry meadow communities from the Saddle (control) simulations with CLM. Growing season (GS) was defined where simulated GPP > 0. All values are means calculated from simulations over the alpine flux tower observational record (2008-2021). DOY stands for day of calendar year.

	Max. snow depth (m)	1st snow free DOY	GS length (days)	GPP (g C m^{-2} y^{-1})	Peak runoff DOY	GS soil moisture (%)	GS soil temp. (˚C)
Moist	1.47	185	104.2	350.3	156	29.6	13.5
Wet	0.98	184	109.6	569.0	153	32.7	11.7
Dry	0.12	175	129.5	201.4	105	27.6	15.0

Modifications to winter precipitation allowed CLM simulations to capture observed gradients in snow accumulation across moist, wet, and dry meadows, as intended. Maximum snow depths simulated in each community (1.47 ± 0.55 m, 0.98 ± 0.36 m, and 0.12 ± 0.04 m in moist, wet, and dry meadow, respectively) corresponded well with observations across the Saddle grid (Table 1; Figure 2a-c). The simulations also captured interannual variability in snowpack across the 14-year measurement record (Figure S1). We found early biases in the timing of peak snow depth, initiation of snowmelt, and the first snow free day compared to

observations (Figure 2a-c). The first snow free day was ~20-30 days early in the moist and wet meadows, but values in the dry meadow matched observations more closely (Figure 2, Table 1).

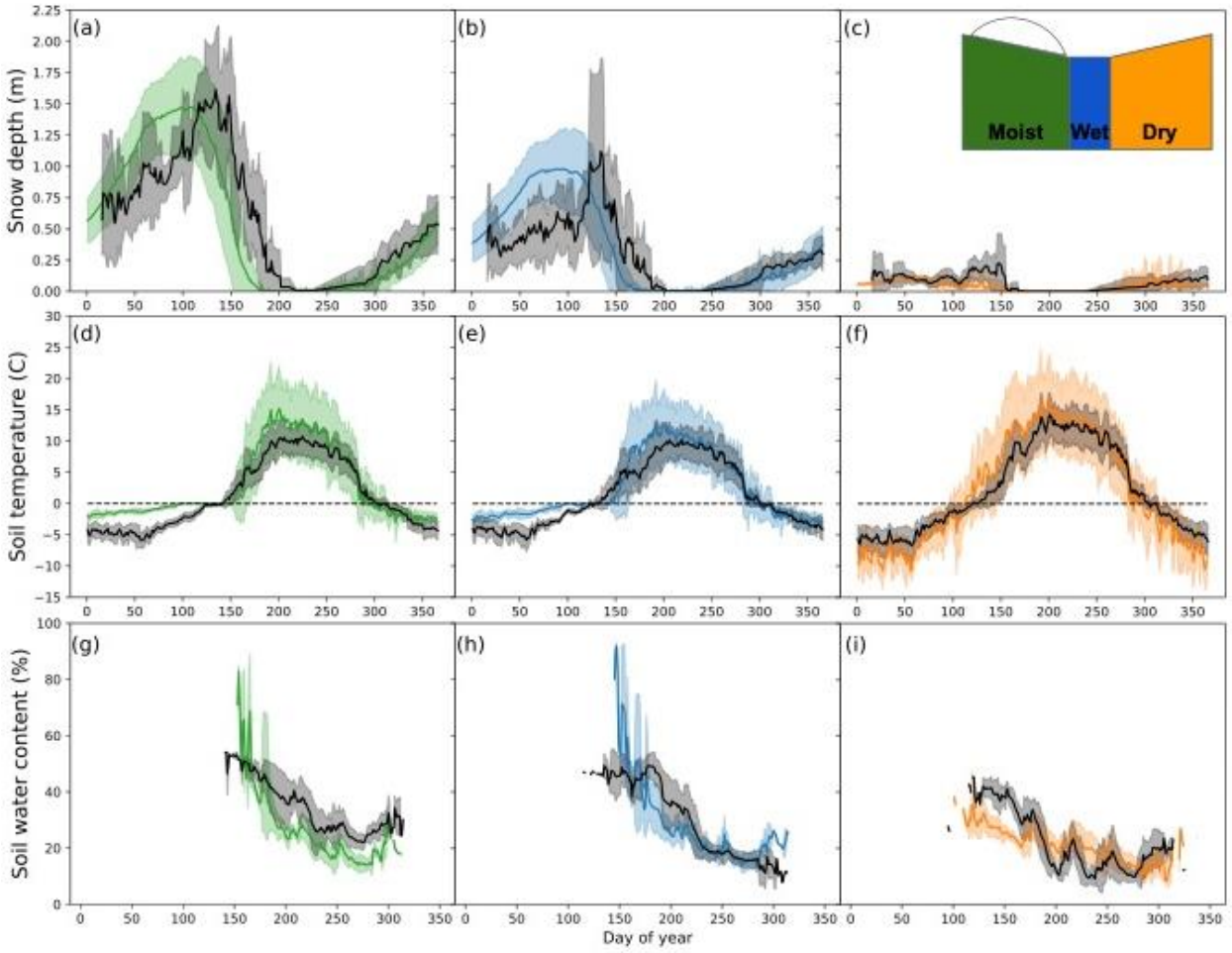

Figure 2. Annual climatology of mean daily (± SD) (a-c) snow depth, (d-f) soil temperature (4 cm depth), and (g-i) soil water content (4 cm depth; when soil temp. > 0) from CLM simulations configured for moist, wet, and dry meadow communities. Simulations and observations were averaged by day of year across 2008-2021 (snow depth) or 2017-2021 (soil temperature and water content) for each community, with dry, moist, and wet meadows in orange, green, and blue lines, respectively, and observations in black.

Differences in timing between observations and simulations are unsurprising given the spatially and temporally variable nature of snow observations, which are particularly difficult to measure at high altitude sites with high wind transport (Williams et al., 1998). While CLM does not account for blowing snow, our simplified precipitation modifications resulted in a dry meadow snowpack that was thin and variable throughout the winter, as in the observations;

however, the simulations underestimated the effects of late spring storms, when heavier, higher-moisture snow can accumulate in windblown areas (Figure 2c). Early melt biases may also point to known shortcomings in the radiative transfer and albedo representation of snow in CLM. Indeed, proposed updates to the Snow, Ice, and Aerosol Radiative (SNICAR) module (Flanner et al., 2021) used in CLM offer promise–but additional work is needed to evaluate this scheme, which is outside the scope of this work. Our findings show that vegetation in CLM experiences snow-free conditions earlier in the growing season than actual plant communities at Niwot Ridge typically experience, but since soil temperature controls phenology for CLM Arctic C_3 grasses, the representation of soil temperature may be more important to consider than snow-free date.

Soil temperature and moisture simulated by the CLM broadly captured the climatological patterns observed among moist, wet, and dry meadows (Figure 2d-i), as well variation as between years (Figure S2). During winter months, moist and wet meadow soils remained near freezing due to the insulating effect of the snowpack, whereas snow-free dry meadow soils remained well below freezing. During the spring and summer, moist and wet meadow soils warmed later in the growing season (consistent with later snowmelt) and experienced lower maximum soil temperatures. By contrast, dry meadow soils warmed quickly in spring, resulting in a longer growing season with higher maximum summer temperatures (Table 1; Figure 2d-f). We found a bias towards warmer simulated soil temperatures (both winter and summer), notably in the moist and wet meadows (Figure 2d-e). Winter biases likely occurred due to the development of a deeper early season snowpack in moist and wet communities in CLM compared to observations (Figures 2a, 2b, and S1). Work at other sites suggests that snow thermal conductivity in CLM5 is too high, resulting in cold wintertime soil temperature biases (Dutch et al., 2022; Luo et al., 2023). Preliminary results from our simulations at Niwot Ridge,

however, suggest that thermal conductance of snow may be too low, resulting in warm winter soil temperature biases in moist and wet meadow columns.

Mean soil moisture (when soil temperatures were above 0˚C) averaged 44.2 ± 13.6%, 45 ± 12.6%, and 31.7 ± 6.2% in moist, wet, and dry meadows, respectively, with moist and wet meadow soils maintaining higher soil moisture longer in the growing season than dry meadow soils (Figure 2g-i). As in previous modeling efforts at Niwot Ridge (Wieder et al., 2017), moist meadow soil moisture was primarily driven by snowmelt, whereas wet meadow soils received additional water subsidies from upslope areas, allowing them to maintain more moisture during the growing season (Figure 2g, 2h, and Table 1). By contrast, dry meadow soil moisture closely tracked episodic summer rainfall events (Figures 2i and S2f). In moist meadow sites, our simulations showed biases toward low soil moisture compared to observations. This could reflect a feedback between simulated soil hydrology and plant physiology, as higher than observed moist meadow productivity (Figure 3) may concurrently dry out soils in the model. Moreover, the soil hydraulic properties used in CLM may allow excess drainage in moist meadow soils and subsequent transfers to downslope wet meadow columns (although wet meadow soil moisture was also underestimated at this site). Meanwhile, in the dry meadow, CLM was unable to capture both the moisture peak following snowmelt and the magnitude of dry down throughout the growing season. Additional modifications to input data may better capture the late spring storms that led to deeper dry-meadow snow in the observations compared to our results (Figure 2c) and may improve dry meadow soil moisture early in the growing season. Moreover, our column-specific modifications to better represent rocky alpine soils (Table S1) in CLM may warrant further investigation for studies seeking higher fidelity simulations of soil abiotic conditions.

Broadly, our findings underscore the challenges of representing biophysical and biogeochemical processes in sophisticated land models with high dimensionality parameter space (Dagon et al., 2020). For example, the generalized pedotransfer functions that are used in global scale, coarse resolution climate simulations with CLM may need more careful evaluation for local application in ecosystem-scale studies (Dai et al., 2019; Luo et al., 2023). Such detailed measurements of soil thermal and hydraulic properties, however, are not commonly collected in sites with co-located measurements of plant traits (for model parameterization) and long-term measurements of ecosystem fluxes (for model calibration and evaluation). Indeed, even at a well-studied site such as Niwot Ridge, a paucity of data on soil physical properties precludes more robust interrogation of the belowground biases in our simulations. Moreover, the continuous, distributed measurements of soil temperature and moisture that we present are relatively new additions to the LTER data collections that began in 2018, following previous data-model integrations by Wieder et al. (2017). Given the harsh alpine environment, these data are hard-earned but likely inadequate to capture the high variability that characterizes soil moisture conditions across complex terrain (Loescher et al., 2014). Despite these challenges, our results demonstrate that the hillslope hydrology configuration of CLM can broadly represent meaningful abiotic conditions and ecological functions across a heterogeneous landscape.

Simulated estimates of both GPP and ANPP increased with moisture and snow depth across the tundra hillslope gradient (Figure 3 and Table 1), with mean annual GPP averaging 350 ± 45, 569 ± 51, and 201 ± 21 g C m^{-2} yr^{-1} in moist, wet, and dry meadow columns, respectively. Although moist meadow communities had the deepest snowpack, they were less productive than the wet meadow due to a shorter growing season (Figure 3 and Table 1). Wet meadow communities receive water subsidies from uphill columns, largely the moist meadow, and

experience little to no water stress during the growing season. On the other hand, dry meadow experiences the longest growing season and highest soil temperatures, but water limitation leads to more conservative growth strategies in this community (Spasojevic & Suding, 2012; Winkler et al., 2018). While simulated GPP values in the dry meadow were higher on average than the alpine flux tower observations (Figure 3b), they fell within the range of uncertainty, indicating that our simulations provide reasonable estimates of productivity (Figure 3a). Moreover, the footprint of the alpine flux towers includes significant areas of fellfield vegetation, which is heavily snow-scoured with very shallow, poorly developed soils, sparse vegetation cover, and lower productivity than dry meadow (Burns, 1980; Knowles et al., 2016; Wieder et al., 2017).

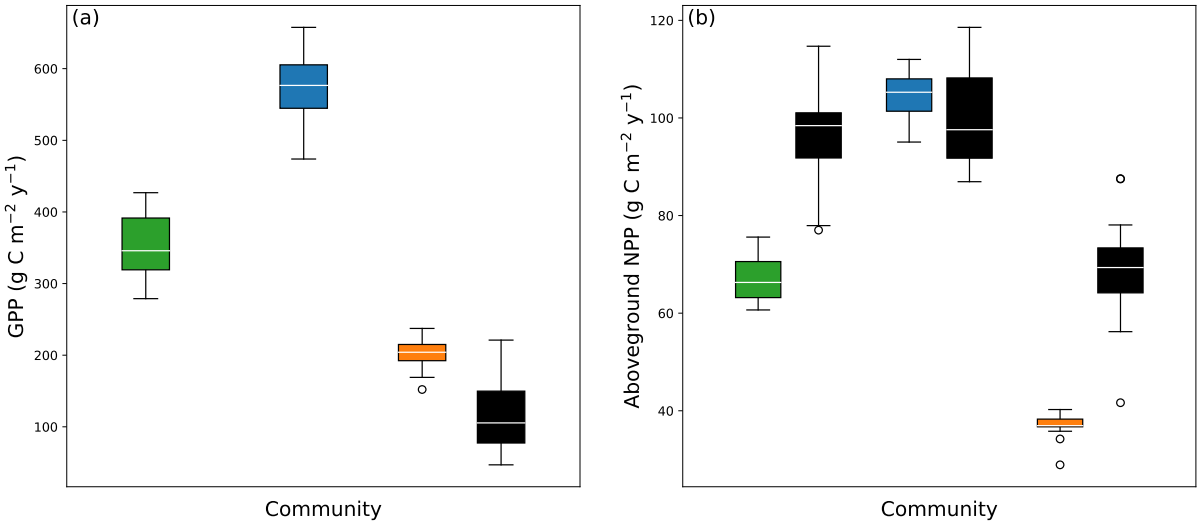

Figure 3. Boxplots of observed vs. simulated (a) mean annual gross primary productivity (GPP) and (b) aboveground net primary productivity (ANPP). Green, blue, and orange denote CLM simulations of moist, wet, and dry meadow communities, respectively, and black denotes observations from alpine flux towers (GPP, dry meadow only) and biomass harvests from the Saddle (ANPP), Niwot Ridge. Boxplot parameters throughout are as follows: median (white lines), interquartile range (boxes), and 1.5x interquartile range (whiskers).

Without community-specific estimates of GPP, we calibrated model parameters to simulate differences in ANPP among vegetation communities, which our results broadly captured (Figure 3b). We found that the model underestimated ANPP by ~30 g C m^{-2} yr^{-1} in moist and dry meadows compared to long-term measurements in the Saddle. A number of

parameters could be responsible for these biases. For example, compared to the default parameter in CLM5, we increased fine root C allocation relative to leaf C allocation, (Table S1), a modification supported by literature that demonstrates higher belowground C investment in arctic and alpine plants (Birch et al., 2021; Iversen et al., 2015; Jackson et al., 1996). Further modifications to the parameterizations of photosynthetic capacity, plant hydraulic stress, nutrient use efficiency, allocation, and turnover could further refine these results. Indeed, such efforts are the focus of ongoing work. Future work, therefore, should focus on quantifying broad plant functional traits for alpine vegetation and characterizing different growth strategies within and among tundra communities (Sulman et al., 2021). Broadly, however, our hillslope implementation of CLM5 adequately captured gradients in snow accumulation and ablation, soil temperature and moisture, and productivity that are observed among moist, wet, and dry meadow communities at Niwot Ridge. Next, we apply this modeling framework to investigate how aspect mediates ecosystem function in alpine tundra systems.

3.2 Model application: Aspect controls on hydrology, soil conditions, and growing season length

Leveraging novel capabilities of the hillslope hydrology configuration in CLM, we applied our modeling framework to investigate potential aspect-driven differences across topographically complex alpine landscapes. These north and south aspect simulations had the expected effect of decreasing snow depth on south aspects (Figure 4a-c and Table 2), indicating that higher winter solar radiation on south-facing slopes increases sublimation. During the spring, however, higher solar zenith angles reduce aspect-driven differences in solar radiation, which is the primary driver of ablation. Thus, our simulations showed negligible differences in

the timing of snowmelt between north- and south-facing simulations. Under current (2008-2021) conditions, only the moist meadow experienced delays in the first snow free day on north aspects compared to south aspects (Table 2). Deeper snowpack in the north aspect, however, did alter the timing and magnitude of runoff fluxes and transfers between hillslope columns. Peak runoff occurred later in north-facing columns, particularly in the wet meadow, which receives water subsidies from uphill moist meadow columns (Table 2; Figure 4d-f).

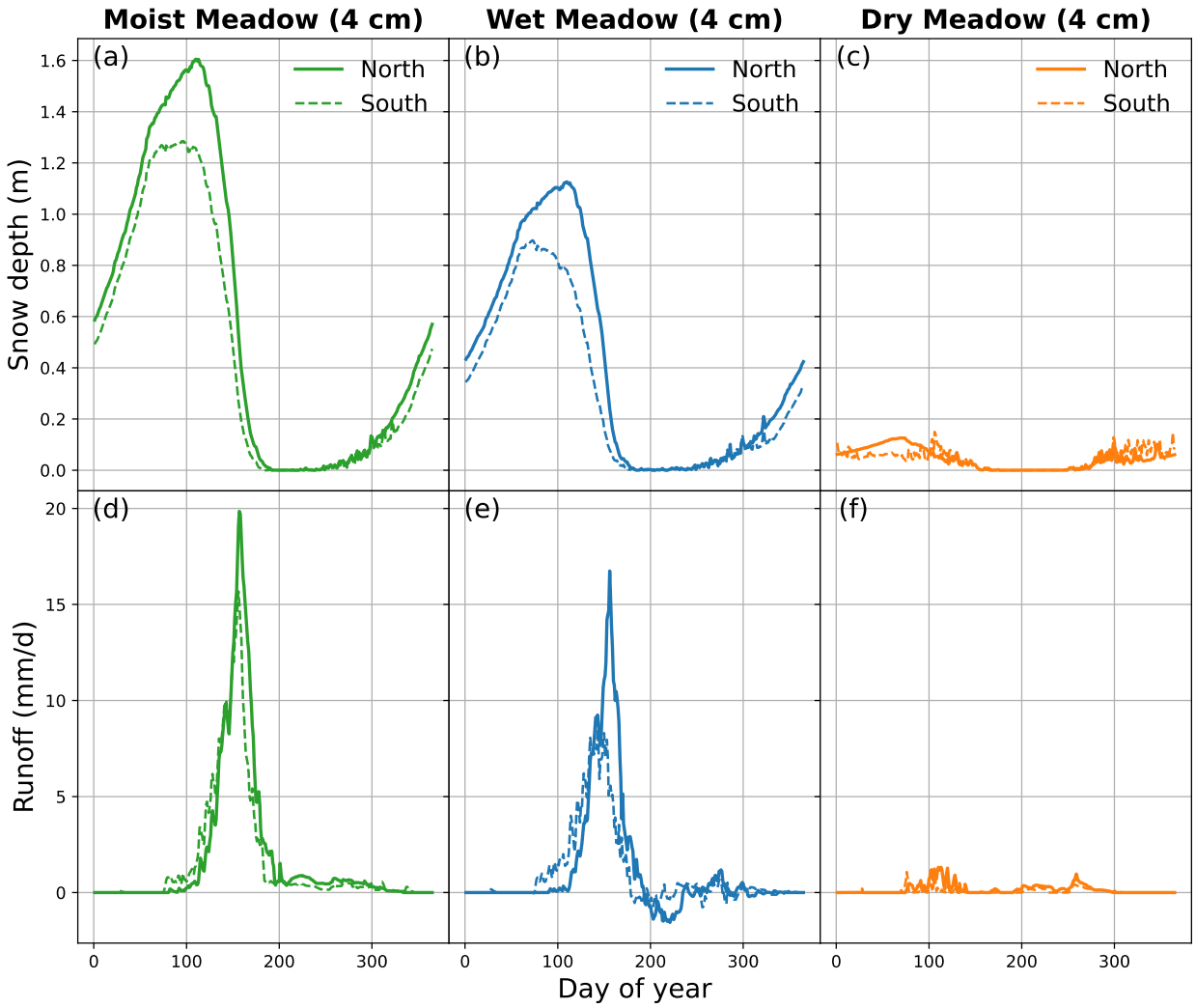

Figure 4. Mean annual climatology of snow depth (a-c) and runoff (d-f) from CLM simulations configured for north (solid lines) and south (dashed lines) aspects with moist (green lines), wet (blue lines), and dry (orange lines) meadow vegetation. Results were averaged by day of year across 2008-2021 study period for each community and aspect. Negative runoff values occur when inflow from uphill is greater than outflow.

Despite similarities in snowmelt timing, we found that south aspects had longer growing seasons in all three communities (defined as the number of days when simulated GPP > 0). This occurred because south-facing soils warmed earlier than north-facing soils experiencing wetter, cooler conditions (Figure 5). Throughout the growing season, north-facing soils were 2.9, 3.5, and 2.2 ˚C cooler and 3.8, 3.8, and 4.2% wetter than south-facing soils in moist, wet, and dry meadows, respectively (Table 2), but the annual cycle of these differences varied (Figure 5). Specifically, the deep moist meadow snowpack buffered soils from aspect-driven differences in winter solar radiation, leading to negligible differences in winter soil temperatures between aspects (Figure 5a). Meanwhile, the dry meadow lacked this snow insulation and experienced warmer winter soil temperatures on south aspects (Figure 5c). Although south aspects had drier soils throughout the year, annual cycles of soil moisture were consistent between aspects in moist and dry meadows (Figure 5d, f). In contrast, the wet meadow had almost no aspect-driven difference in soil moisture early in the growing season, when runoff from the uphill moist meadow provided supplementary water inputs (Figure 4e); however, after day ~210 (late July), aspect effects emerged when south-facing soils dried out faster (Figure 5b). Overall, these differences in soil moisture and temperature highlight the role of aspect in controlling abiotic conditions across heterogeneous alpine environments (Isard, 1986), with implications for plant community composition and function. For example, in a subarctic forest-tundra ecotone, aspect was a stronger control on community composition than slope angle or elevation, driven by increased soil temperature and active layer depth (Dearborn & Danby, 2017). Similarly, our results suggest that historical snow accumulation patterns influence subsequent aspect-driven differences in soil temperature and moisture that may moderate how tundra vegetation experiences warming across heterogeneous alpine terrain.

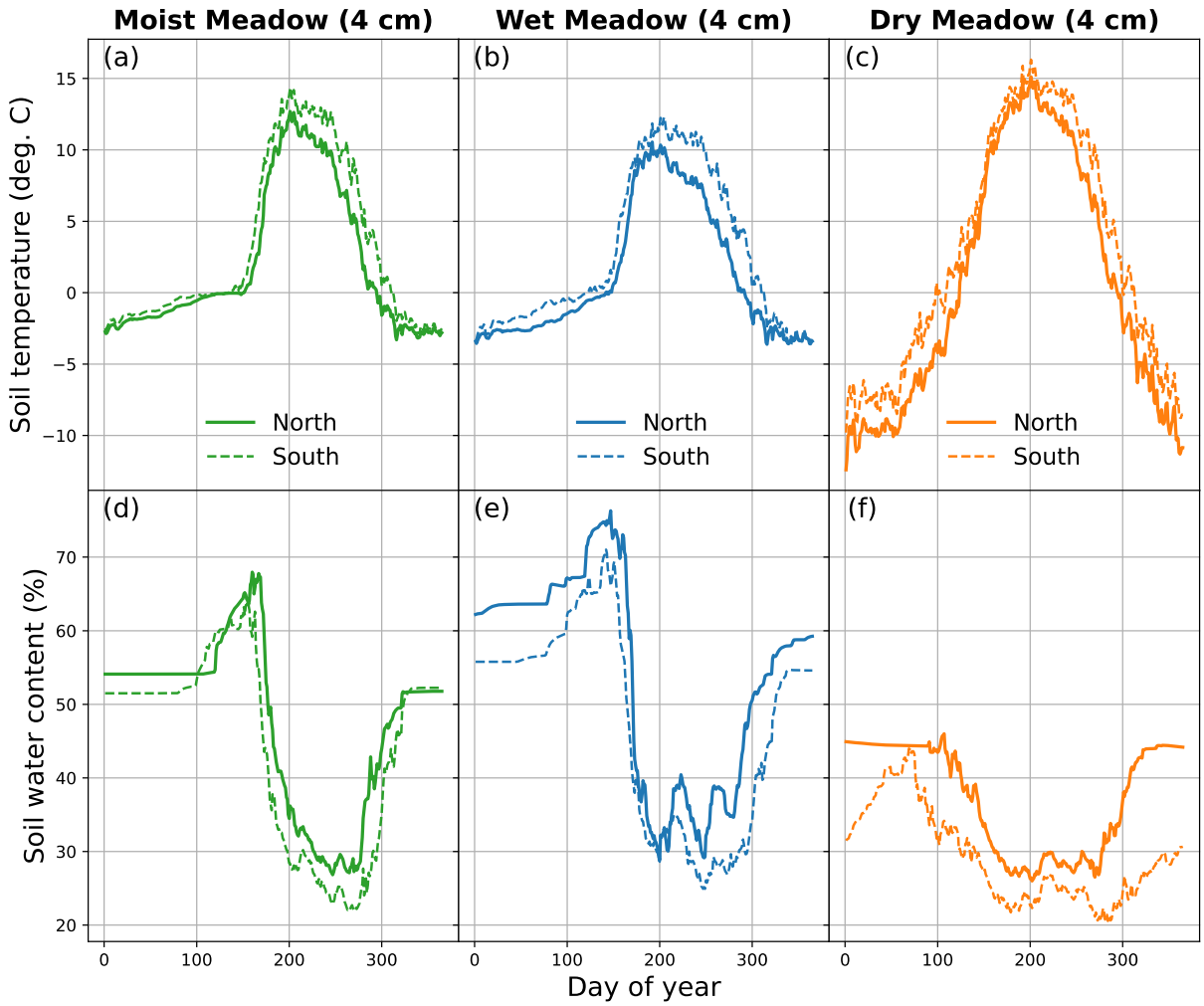

Figure 5. Mean annual climatology of soil temperature (a-c) and volumetric soil water content (d-f) at 4 cm depth from CLM simulations configured for north (solid lines) and south (dashed lines) aspects with moist (green lines), wet (blue lines), and dry (orange lines) meadow vegetation. Results were averaged by day of year across 2008-2021 study period for each community-aspect pairing.

Previous work on the impacts of topographic relief at hillslope scales indicates that warmer slopes should support longer growing seasons in areas with energy limitation, while cooler slopes can support higher productivity in areas with water limitation (Fan et al., 2019). Given that in our simulations, south aspects had longer growing seasons than north aspects (7-8% longer depending on community; Table 2), differences in cumulative GPP were surprising. Because moist meadow vegetation experiences a short growing season (May et al., 1982), we expected south aspects to have higher productivity, which was true, but only slightly (Figure

518 S3g, S3h; Table 2). These results align with the marginally earlier snowmelt date, higher soil
519 temperature, and lower soil moisture conditions that characterized south-facing simulations
520 (Figures 4-5). By contrast, north aspects were more productive in both wet (Figure 6g, 6h) and
521 dry meadows (Figure S4g, S4h and Table 2). We suspect that growing season length is less
522 limiting of wet and dry meadow, with soil N and water, respectively, providing larger constraints
523 in CLM (as in Wieder et al. 2017). Moreover, the increase in wet and dry meadow productivity
524 on north aspects may be a result of lower soil temperatures (Figure 5b) that reduce maintenance
525 respiration (thereby increasing plant C use efficiency) or plant-soil feedbacks resulting from
526 higher soil N stocks due to higher soil organic matter content simulated on north-facing slopes,
527 which is also consistent with observations (Egli et al., 2009; Spasojevic et al., 2014).
528
529 3.3 Model projections: Alpine tundra responses to simulated warming and increased CO_2
530 To examine the role of microsite variation in potentially buffering alpine vegetation
531 against climate change, we extended our simulations to year 2100 for all three communities on
532 north- and south-facing aspects. The anomaly forcing from CESM2 included a 3.5˚C warming of
533 air temperature and an 8.2% increase in precipitation by 2100, relative to the historical baseline.
534 These projected climate changes drove shifts in the timing of snow accumulation and ablation
535 that had cascading effects on soil temperature, plant water availability, and productivity patterns,
536 but the magnitude of these effects varied with landscape position. For brevity, we illustrate
537 climate change effects on wet meadow columns (Figure 6), and present moist and dry meadow
538 results in Table 2 and supplementary material (Figures S3-S4).

539 **Table 2.** Comparison of key metrics related to snow, water, productivity, and soil conditions
540 between moist, wet, and dry meadow communities across north (N) and south (S) aspects for
541 historical (2008-2021) and future (2086-2099) simulations. Growing season (GS) was defined
542 where GPP > 0. DOY stands for day of calendar year.

Experiment			Max. snow depth (m)	1st snow free DOY	GS length (days)	GPP (g C m^{-2} y^{-1})	Peak runoff DOY	GS soil moisture (%)	GS soil temp. (˚C)
Moist	**S**	**Historical**	1.28	184	107	363	155	28.7	14.8
		Future	1.27	165	125	631	135	26.8	17.6
	N	**Historical**	1.61	197	100	342	156	32.5	11.9
		Future	1.6	174	113	595	140	28.1	15.4
Wet	**S**	**Historical**	0.9	184	112	516	142	31.1	12.8
		Future	0.85	164	126	857	127	34.2	15.6
	N	**Historical**	1.13	184	105	628	155	35.0	9.4
		Future	1.1	164	115	997	142	33.3	13.0
Dry	**S**	**Historical**	0.15	167	137	241	105	24.2	15.4
		Future	0.16	152	150	403	69	21.3	18.4
	N	**Historical**	0.13	167	126	259	112	28.5	13.2
		Future	0.11	146	134	418	75	24.9	16.5

With projected warming, we found that the timing of snowmelt and runoff shifted earlier across all simulations, with concurrent decreases in maximum runoff rates. While maximum snow depth changed little between historical and future scenarios, the snowpack melted earlier in all future simulations (by 15-23 days depending on community and aspect; Table 2), leading to an 8-18% increase in growing season length, depending on location. Peak runoff was generally reduced and occurred earlier for all communities and aspects in future simulations (13-37 days earlier, with smaller and larger changes in wet meadow and dry meadows, respectively; Table 2), shifting the timing of runoff earlier relative to the start of the growing season (Figures 6c, 6d, S3c, S3d, S4c, and S4d). These changes in runoff timing and magnitude align with expectations and with previous modeling studies predicting that shallower snowpacks will melt earlier and more slowly across the Western U.S. (Clow, 2010; Musselman et al., 2017). However, an exception to the pattern of reduced runoff occurred in the south facing wet meadow, where peak runoff was approximately 20% higher in the future scenario (Figure 6c), peaking more quickly and being followed by a more rapid decline compared to the historical scenario. This increase

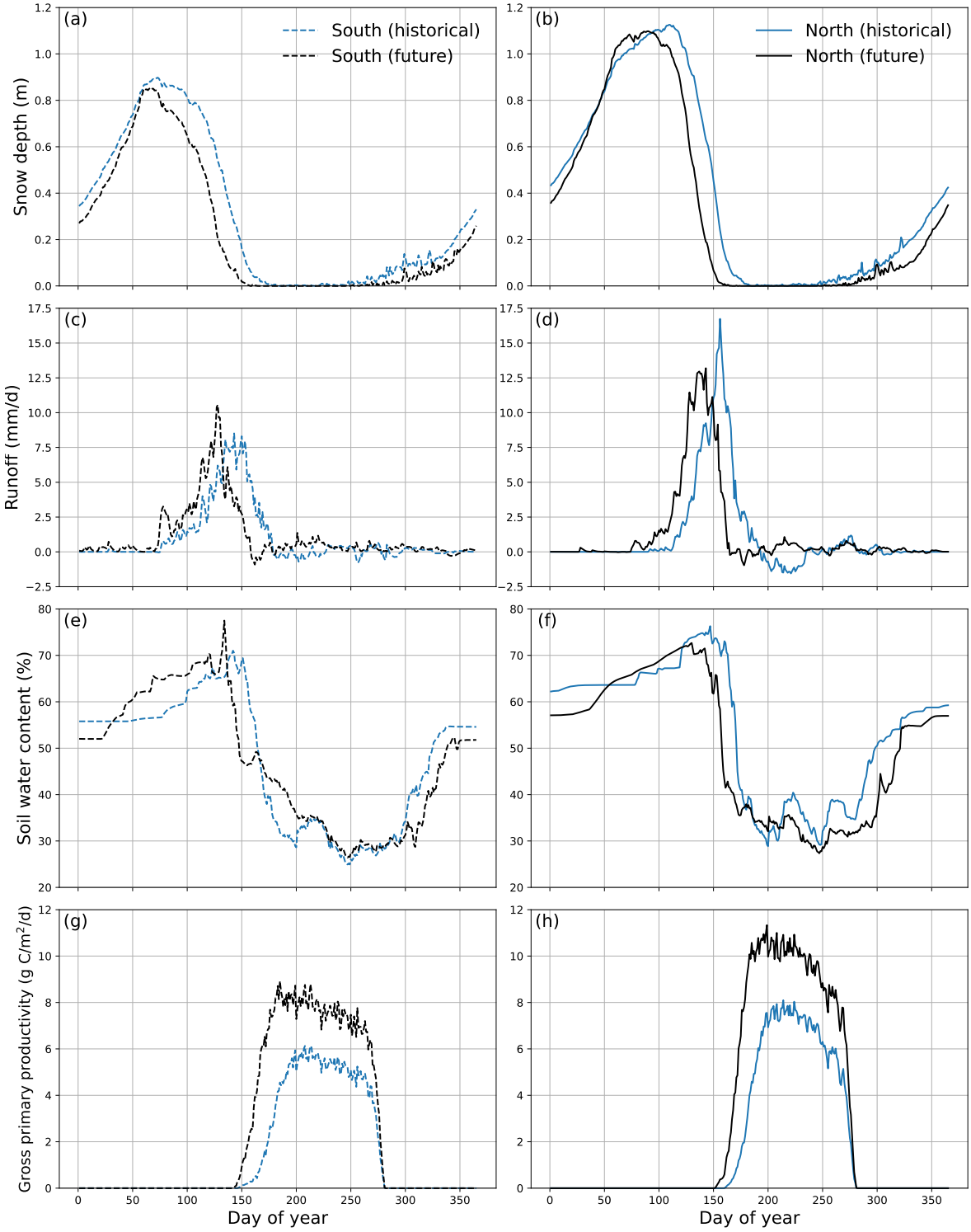

Figure 6. Mean annual climatology of (a, b) snow depth (m), (c, d) runoff (mm/d), (e, f) soil moisture (%), and (g, h) productivity in the wet meadow (lowland) column for historical (blue lines; 2008-2021) and future (black lines; 2086-2099) time periods. Results from south aspect (dashed lines) are shown in left column and those from north aspect (solid lines) are in right column. Values were averaged by day of year for each scenario and aspect. Negative runoff values occur when inflow from uphill is greater than outflow.

565 may be explained by a combination of factors including moist meadow water subsidies being
566 passed downslope earlier (Figure S3), increased surface runoff due to lack of infiltration of
567 snow-covered soils (Evans et al., 2018), and complex feedbacks between snow ablation rates,
568 evapotranspiration, and plant water use (Barnhart et al., 2020; Harpold & Brooks, 2018).

569 Shifts in the timing and magnitude of snowmelt and runoff in our simulations suggest that
570 plants are likely to experience decreased growing season water availability when demand is high,
571 ultimately increasing plant water stress. These findings are consistent with previous modeling
572 efforts at Niwot Ridge (Dong et al., 2019; Wieder et al., 2017) and measurements in a high-
573 elevation Colorado wetland (Blanken, 2014). Seasonal snowmelt in alpine regions provides
574 critical water resources in the Western U.S., but these high-elevations areas are particularly
575 susceptible to climate change (Immerzeel et al., 2020; Mote et al., 2005). Water balance
576 measurements in headwater catchments including Niwot Ridge have shown disproportionately
577 high contributions of alpine tundra areas to total catchment discharge (Knowles et al., 2015),
578 suggesting that these shifts in snowpack and runoff have significant implications for downstream
579 water resources and hydrological processes.

580 Differences in the timing of snowmelt and runoff in our simulations led to shifts in
581 growing season soil moisture and plant productivity across the hillslope gradient. In the moist
582 and dry meadows, soils were consistently drier throughout the growing season in the future
583 simulations (Figures S3e, S3f and S4e, S4f, Table 2). Indeed, dry meadow soil moisture patterns
584 largely reflected episodic summer precipitation events, consistent with observations at the site
585 (Figure 2i). The anomaly forcing approach we used cannot address potential changes in monsoon
586 variability or strength that may be associated with climate change (Pascale et al., 2017), but our
587 results underscore the importance of summer precipitation in determining plant water availability

588 in dry, and even moist meadow ecosystems. By contrast, because they received water subsidies
589 from upslope, wet meadow soils were relatively buffered from changes in growing season soil
590 moisture (Figure 6e and 6f). This finding is supported by previous work at Niwot Ridge
591 emphasizing the role of snowmelt in shaping soil moisture in wetter areas (Taylor & Seastedt,
592 1994). We also found increased GPP in all communities in tandem with earlier snowmelt, drier
593 soils, longer growing seasons, and increased atmospheric CO_2 concentrations (Figures 6, S3, and
594 S4), although previous work has shown mixed productivity responses to warmer and drier
595 conditions in tundra systems (Dong et al., 2019; Yang et al., 2020).
596 Simulated shifts in soil temperature and moisture varied with landscape position, with
597 south aspects generally changing more than north aspects. We attributed these shifts to either
598 aspect or community, depending on the metric, indicating that spatial heterogeneity can play a
599 key role in moderating exposure to climate change. For example, south-facing dry meadow
600 vegetation showed the biggest change in annual mean soil temperature and moisture in future
601 simulations (Figure 7a, 7b). These changes in surface soil temperatures tracked the increase in air
602 temperature from 2008-2100 (dashed line; Figure 7a). Previous work by Wentz et al., (2019)
603 found that under current conditions dry meadow leaf temperatures were higher than in other
604 communities and already near optimal values for photosynthesis, concluding that a 2˚C air
605 temperature increase would likely decrease carbon assimilation. In our simulations, dry meadow
606 vegetation temperatures were approximately 1.7˚C and 2.1˚C higher than those in the moist and
607 wet meadows, respectively. Our finding that soil temperatures track air temperatures in dry
608 meadows suggests that these plants are likely more vulnerable to adverse effects of warming
609 from climate change. In contrast, moist and wet meadow surface soil temperatures increased
610 much less than air temperature due to the insulating effect of their deeper snowpack.

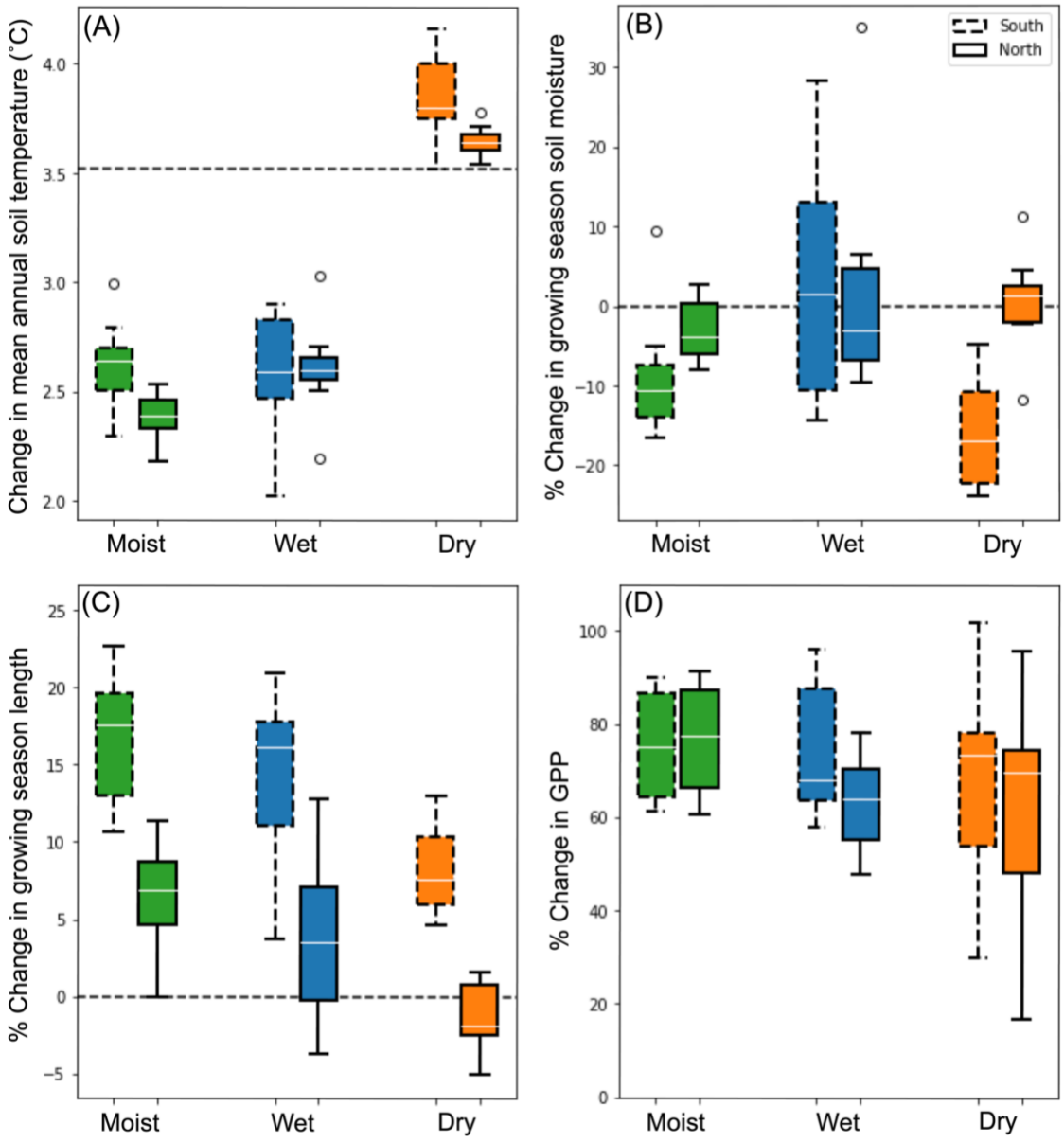

611 **Figure 7.** Metrics of climate change exposure and ecosystem services are moderated by
612 community type and aspect in Niwot Ridge alpine tundra ecosystems. Boxplots show annual
613 mean differences between corresponding years in the historical (2008-2015) and future (2092-
614 2099) time periods for north (solid boxes) and south (dashed boxes) aspects. (a) change in mean
615 annual surface soil temperature (dashed line represents the mean increase in air temperature
616 between 2008 and 2100); (b) percent change in growing season soil moisture (normalized to soil
617 moisture values for each community); (c) percent change in growing season length (normalized
618 to growing season lengths for each community); and (d) percent change in gross primary
619 productivity (normalized to productivity values from each community). Green, blue, and orange
620 boxes represent, moist, wet, and dry communities, respectively.
621

Changes in growing season soil moisture and growing season length were primarily driven by aspect, with smaller differences among communities (Figure 7b-c). Soil moisture in south aspect dry meadow showed the greatest proportional decrease, followed by south aspect moist meadow. Aspect differences in soil moisture were not apparent in the wet meadow, where upslope water subsidies buffered against soil moisture change (Figure 7b). Likewise, increases in growing season length under climate change were more pronounced on south aspects (Figure 7c), with larger increases in moist and wet meadows due to earlier snowmelt (Table 2). Thus, our findings support the role of microclimates in moderating exposure and rates of response to climate change impacts that alpine vegetation may experience, where local conditions experienced by plants can be decoupled from atmospheric changes (Ackerly et al., 2020; Lenoir et al., 2013; Oldfather & Ackerly, 2019). Across the tundra hillslope gradient, differences in snowpack and hydrology dictated responses to warming, where cooler, wetter soils were maintained in lowland vegetation patches that accumulate moisture.

Our results suggest that abiotic shifts driven by changes in snowmelt timing are likely to alter resource connectivity across tundra ecosystems, where shifts in microbial biomass may lead to increased N export during snowmelt and decreased N available to alpine plants. In alpine areas where snow cover and cold soils result in short growing seasons (Billings & Mooney, 1968), lengthening the growing season may have outsized effects on microbial activity, nutrient cycling, and plant community dynamics. Microbial biomass typically peaks under spring snowpack (Lipson et al., 2000; Schadt et al., 2003), and shifts in soil microbial activity, biogeochemical cycling, and microbial community composition occur following snowmelt (Schmidt et al., 2015). For example, high microbial biomass under consistent snow cover buffers against inorganic N export during snowmelt (Brooks et al., 1998), and nutrients released as a result of microbial

activity following snowmelt are a key control on N availability to alpine plants (Lipson et al., 1999). Although our simulations are not well suited to explore these biotic feedbacks, our findings indicate that differences in aspect could moderate exposure to these changes.

In addition to longer growing seasons, we found increased productivity across all future simulations. These changes in GPP varied less between landscape positions than other metrics—all communities and aspects showed mean increases of similar magnitude (Figure 7d). However, GPP increases showed greater interannual variability in the dry meadow, supporting the idea that dry meadow experiences greater exposure to changes in abiotic conditions while moist and wet meadows are more buffered from these changes. In addition to warming effects, these GPP increases reflect greater atmospheric CO_2 concentrations that can lead to higher water use efficiency (Keenan et al., 2013) and higher photosynthetic rates per unit leaf area (Dong et al., 2019), which may help compensate for drier soils under the future climate scenario. In comparison to our findings (GPP increased from ~65-80%), Fan et al., (2016) parameterized an ecosystem biogeochemistry model for dry meadow tundra and found that a 3˚C increase in soil and air temperature led to a corresponding ~50% GPP increase without accounting for increasing atmospheric CO_2. Although we lack observations to evaluate these results, our model evaluation efforts indicate relatively strong agreement between dry meadow simulations and flux tower GPP observations (Figure 3b). Furthermore, studies in arctic and alpine tundra have documented widespread shrubification (Formica et al., 2014; Sturm et al., 2001) and increases in graminoid abundance (Wookey et al., 2009), which tend to be accompanied by increased biomass and productivity and occur in tandem with global change factors. Elsewhere, studies also show that moisture limitation can exert strong controls on tundra productivity (Fan et al., 2016) and shrub growth and recruitment (Mekonnen et al., 2021), suggesting that declines in productivity and

668 shifts in plant community composition may occur in tundra sites experiencing greater soil
669 moisture stress. Though our simulations are not suited to address effects of increased moisture
670 stress on species composition, future efforts could leverage trait databases and ecosystem
671 demography models to improve the representation of alpine plant functional types (Fisher &
672 Koven, 2020) to explore more nuanced productivity responses to environmental change.
673
674 **4 Conclusions**
675 Overall, our findings highlight the value of incorporating site-level measurements into
676 land models to ask ecological questions and improve projections of climate change impacts on
677 ecosystem functions. Using local observations from Niwot Ridge and explicitly incorporating
678 aspect effects on insolation and lateral hydrologic connectivity into our modeling framework, we
679 found that leveraging the hillslope hydrology configuration within CLM allowed us to represent
680 a topographically complex alpine environment. Our simulations captured gradients in snow
681 accumulation, soil temperature and moisture, and productivity among hydrologically connected
682 alpine vegetation communities and allowed us to examine aspect-driven differences and climate
683 warming effects. Our findings demonstrate the role of local scale heterogeneity, including cooler
684 north facing slopes and lowland areas that accumulate moisture, in buffering vegetation from
685 experiencing warming and acting as potential refugia from climate change. Conversely, our
686 findings highlight potential vulnerabilities of vegetation in dry, windblown, and south facing
687 parts of the landscape that are less buffered from environmental change. To better understand
688 how microscale variation will mediate rates of response to warming, future work should aim to
689 better characterize growth strategies and plant functional traits within alpine vegetation and
690 examine how shifts in these traits may mediate tundra responses to change. Interdisciplinary

691 approaches that combine site-level observations with modeling approaches are critical to
692 investigate how rapid warming may alter ecosystem functions and services across
693 topographically complex landscapes.
694
695 **Acknowledgements**
696 This research was supported by NSF grants DEB 1637686 and 2224439 to Niwot Ridge LTER.
697 W. Wieder was also supported by NSF grants 1755088 and 2120804. We thank J. Morse, S.
698 Aplet, and Niwot Ridge staff for project support as well as members of the Suding Lab for
699 helpful discussions and feedback on earlier versions of this manuscript.
700
701 **Open Research**
702 Computing and data storage resources, including the Cheyenne supercomputer
703 (https://doi.org/10.5065/D6RX99HX), were provided by the Computational and Information
704 Systems Laboratory (CISL) at NCAR. Previous and current CLM versions are freely available
705 at: https://www.cesm.ucar.edu/models/clm. The CLM5 data analyzed in this manuscript are in
706 the process of being archived by the NCAR Digital Asset Services Hub
707 (DASH; https://data.ucar.edu) and a doi will be provided when this process is complete. The data
708 are temporarily available for download at:
709 http://ftp.cgd.ucar.edu/pub/wwieder/NWT_CLM_cases.tar.gz. The code used to download data,
710 run analyses, and produce graphics can be found on Zenodo at:
711 https://doi.org/10.5281/zenodo.8083491.

References

Ackerly, D. D., Kling, M. M., Clark, M. L., Papper, P., Oldfather, M. F., Flint, A. L., & Flint, L. E. (2020). Topoclimates, refugia, and biotic responses to climate change. *Frontiers in Ecology and the Environment*, *18*(5), 288–297. https://doi.org/10.1002/fee.2204

Alexander, J. M., Chalmandrier, L., Lenoir, J., Burgess, T. I., Essl, F., Haider, S., et al. (2018). Lags in the response of mountain plant communities to climate change. *Global Change Biology*, *24*(2), 563–579. https://doi.org/10.1111/gcb.13976

Ali, A. A., Xu, C., Rogers, A., Fisher, R. A., Wullschleger, S. D., Massoud, E. C., et al. (2016). A global scale mechanistic model of photosynthetic capacity (LUNA V1.0). *Geoscientific Model Development*, *9*(2), 587–606. https://doi.org/10.5194/gmd-9-587-2016

Barnhart, T. B., Tague, C. L., & Molotch, N. P. (2020). The Counteracting Effects of Snowmelt Rate and Timing on Runoff. *Water Resources Research*, *56*(8), e2019WR026634. https://doi.org/10.1029/2019WR026634

Billings, W. D., & Mooney, H. A. (1968). The ecology of arctic and alpine plants. *Biological Reviews*. Retrieved from https://onlinelibrary.wiley.com/doi/abs/10.1111/j.1469-185X.1968.tb00968.x

Birch, L., Schwalm, C. R., Natali, S., Lombardozzi, D., Keppel-Aleks, G., Watts, J., et al. (2021). Addressing biases in Arctic–boreal carbon cycling in the Community Land Model Version 5. *Geoscientific Model Development*, *14*(6), 3361–3382. https://doi.org/10.5194/gmd-14-3361-2021

Blanken, P. D. (2014). The effect of winter drought on evaporation from a high-elevation wetland. *Journal of Geophysical Research: Biogeosciences*, *119*(7), 1354–1369. https://doi.org/10.1002/2014JG002648

735 Bonan, G. B., Lawrence, P. J., Oleson, K. W., Levis, S., Jung, M., Reichstein, M., et al. (2011).
736 Improving canopy processes in the Community Land Model version 4 (CLM4) using
737 global flux fields empirically inferred from FLUXNET data. *Journal of Geophysical*
738 *Research: Biogeosciences*, *116*(G2), 1–22. https://doi.org/10.1029/2010JG001593
739 Brooks, P. D., Williams, M. W., & Schmidt, S. K. (1998). Inorganic nitrogen and microbial
740 biomass dynamics before and during spring snowmelt. *Biogeochemistry*, *43*(1), 1–15.
741 https://doi.org/10.1023/A:1005947511910
742 Bueno de Mesquita, C. P., White, C. T., Farrer, E. C., Hallett, L. M., & Suding, K. N. (2021).
743 Taking climate change into account: Non-stationarity in climate drivers of ecological
744 response. *Journal of Ecology*, *109*(3), 1491–1500. https://doi.org/10.1111/1365-
745 2745.13572
746 Burns, S. F. (1980). *Alpine soil distribution and development, Indian Peaks, Colorado Front*
747 *Range,*. University of Colorado, Boulder, CO.
748 Burns, S. P., Maclean, G. D., Blanken, P. D., Oncley, S. P., Semmer, S. R., & Monson, R. K.
749 (2016). The Niwot Ridge Subalpine Forest US-NR1 AmeriFlux site – Part 1: Data
750 acquisition and site record-keeping. *Geoscientific Instrumentation, Methods and Data*
751 *Systems*, *5*(2), 451–471. https://doi.org/10.5194/gi-5-451-2016
752 Caine, N. (1996). Streamflow patterns in the alpine environment of North Boulder Creek,
753 Colorado Front Range. *Streamflow Patterns in the Alpine Environment of North Boulder*
754 *Creek, Colorado Front Range*, (104), 27–42.
755 Chen, Y., Wieder, W. R., Hermes, A. L., & Hinckley, E.-L. S. (2020). The role of physical
756 properties in controlling soil nitrogen cycling across a tundra-forest ecotone of the

Colorado Rocky Mountains, U.S.A. *CATENA*, *186*, 104369. https://doi.org/10.1016/j.catena.2019.104369

Christianson, K. R., Loria, K. A., Blanken, P. D., Caine, N., & Johnson, P. T. J. (2021). On thin ice: Linking elevation and long-term losses of lake ice cover. *Limnology and Oceanography Letters*, *6*(2), 77–84. https://doi.org/10.1002/lol2.10181

Clow, D. W. (2010). Changes in the timing of snowmelt and streamflow in Colorado: A response to recent warming. *Journal of Climate*, *23*(9), 2293–2306. https://doi.org/10.1175/2009JCLI2951.1

Dagon, K., Sanderson, B. M., Fisher, R. A., & Lawrence, D. M. (2020). A machine learning approach to emulation and biophysical parameter estimation with the Community Land Model, version 5. *Advances in Statistical Climatology, Meteorology and Oceanography*, *6*, 223–244. https://doi.org/10.5194/ascmo-6-223-2020

Dai, Y., Xin, Q., Wei, N., Zhang, Y., Shangguan, W., Yuan, H., et al. (2019). A global high-resolution data set of soil hydraulic and thermal properties for land surface modeling. *Journal of Advances in Modeling Earth Systems*, *11*(9), 2996–3023. https://doi.org/10.1029/2019MS001784

Danabasoglu, G., Lamarque, J. -F., Bacmeister, J., Bailey, D. A., DuVivier, A. K., Edwards, J., et al. (2020). The Community Earth System Model Version 2 (CESM2). *Journal of Advances in Modeling Earth Systems*, *12*(2). https://doi.org/10.1029/2019MS001916

Daubenmire, R. F. (1943). Vegetational Zonation in the Rocky Mountains. *Botanical Review*, *9*(6), 325–393.

Dearborn, K. D., & Danby, R. K. (2017). Aspect and slope influence plant community composition more than elevation across forest–tundra ecotones in subarctic Canada. *Journal of Vegetation Science*, *28*(3), 595–604.

Dong, Z., Driscoll, C. T., Campbell, J. L., Pourmokhtarian, A., Stoner, A. M. K., & Hayhoe, K. (2019). Projections of water, carbon, and nitrogen dynamics under future climate change in an alpine tundra ecosystem in the southern Rocky Mountains using a biogeochemical model. *Science of The Total Environment*, *650*, 1451–1464. https://doi.org/10.1016/j.scitotenv.2018.09.151

Dutch, V. R., Rutter, N., Wake, L., Sandells, M., Derksen, C., Walker, B., et al. (2022). Impact of measured and simulated tundra snowpack properties on heat transfer. *The Cryosphere*, *16*(10), 4201–4222. https://doi.org/10.5194/tc-16-4201-2022

Egli, M., Sartori, G., Mirabella, A., Favilli, F., Giaccai, D., & Delbos, E. (2009). Effect of north and south exposure on organic matter in high alpine soils. *Geoderma*, *149*(1), 124–136. https://doi.org/10.1016/j.geoderma.2008.11.027

Elwood, K. K., Smith, J. G., Elmendorf, S. C., & Niwot Ridge LTER. (2022). *Time-lapse camera (phenocam) imagery of sensor network plots, 2017 - ongoing. ver 3*. Environmental Data Initiative. Retrieved from https://doi.org/10.6073/pasta/285918fbf5cc4bd2ed2c1241db9a1b2d

Erickson, T. A., Williams, M. W., & Winstral, A. (2005). Persistence of topographic controls on the spatial distribution of snow in rugged mountain terrain, Colorado, United States. *Water Resources Research*, *41*(4). https://doi.org/10.1029/2003WR002973

Ernakovich, J. G., Hopping, K. A., Berdanier, A. B., Simpson, R. T., Kachergis, E. J., Steltzer, H., & Wallenstein, M. D. (2014). Predicted responses of arctic and alpine ecosystems to

altered seasonality under climate change. *Global Change Biology*, *20*(10), 3256–3269. https://doi.org/10.1111/gcb.12568

Evans, S. G., Ge, S., Voss, C. I., & Molotch, N. P. (2018). The role of frozen soil in groundwater discharge predictions for warming alpine watersheds. *Water Resources Research*, *54*(3), 1599–1615. https://doi.org/10.1002/2017WR022098

Fan, Y., Clark, M., Lawrence, D. M., Swenson, S., Band, L. E., Brantley, S. L., et al. (2019). Hillslope hydrology in global change research and Earth System Modeling. *Water Resources Research*, *55*(2), 1737–1772. https://doi.org/10.1029/2018WR023903

Fan, Z., Neff, J. C., & Wieder, W. R. (2016). Model-based analysis of environmental controls over ecosystem primary production in an alpine tundra dry meadow. *Biogeochemistry*, *128*(1), 35–49. https://doi.org/10.1007/s10533-016-0193-9

Fisher, R. A., & Koven, C. D. (2020). Perspectives on the future of land surface models and the challenges of representing complex terrestrial systems. *Journal of Advances in Modeling Earth Systems*, *12*(4), e2018MS001453. https://doi.org/10.1029/2018MS001453

Fisk, M. C., Schmidt, S. K., & Seastedt, T. R. (1998). Topographic patterns of above- and belowground Production and nitrogen cycling in alpine tundra. *Ecology*, *79*(7), 2253–2266. https://doi.org/10.1890/0012-9658(1998)079[2253:TPOAAB]2.0.CO;2

Flanner, M. G., Arnheim, J. B., Cook, J. M., Dang, C., He, C., Huang, X., et al. (2021). SNICAR-ADv3: a community tool for modeling spectral snow albedo. *Geoscientific Model Development*, *14*(12), 7673–7704. https://doi.org/10.5194/gmd-14-7673-2021

Formica, A., Farrer, E. C., Ashton, I. W., & Suding, K. N. (2014). Shrub expansion over the past 62 years in Rocky Mountain alpine tundra: Possible causes and consequences. *Arctic,*

Antarctic, and Alpine Research, *46*(3), 616–631. https://doi.org/10.1657/1938-4246-46.3.616

Harpold, A. A., & Brooks, P. D. (2018). Humidity determines snowpack ablation under a warming climate. *Proceedings of the National Academy of Sciences*, *115*(6), 1215–1220. https://doi.org/10.1073/pnas.1716789115

Helm, D. (1982). Multivariate Analysis of Alpine Snow-Patch Vegetation Cover near Milner Pass, Rocky Mountain National Park, Colorado, U.S.A. *Arctic and Alpine Research*, *14*(2), 87–95. https://doi.org/10.1080/00040851.1982.12004285

Hermes, A. L., Wainwright, H. M., Wigmore, O., Falco, N., Molotch, N. P., & Hinckley, E.-L. S. (2020). From Patch to Catchment: A Statistical Framework to Identify and Map Soil Moisture Patterns Across Complex Alpine Terrain. *Frontiers in Water*, *2*, 578602. https://doi.org/10.3389/frwa.2020.578602

Hinckley, E. S., Ebel, B. A., Barnes, R. T., Anderson, R. S., Williams, M. W., & Anderson, S. P. (2012). Aspect control of water movement on hillslopes near the rain– snow transition of the Colorado Front Range. *Hydrological Processes*, *28*(1), 74–85. https://doi.org/10.1002/hyp.9549

Hock, R., Rasul, G., Adler, C., Cáceres, B., Gruber, S., Hirabayashi, Y., et al. (2019). *IPCC special report: High Mountain Areas, IPCC Special Report on the Ocean and Cryosphere in a Changing Climate*.

Hudiburg, T. W., Law, B. E., & Thornton, P. E. (2013). Evaluation and improvement of the Community Land Model (CLM4) in Oregon forests. *Biogeosciences*, *10*(1), 453–470. https://doi.org/10.5194/bg-10-453-2013

Immerzeel, W. W., Lutz, A. F., Andrade, M., Bahl, A., Biemans, H., Bolch, T., et al. (2020). Importance and vulnerability of the world's water towers. *Nature*, *577*(7790), 364–369. https://doi.org/10.1038/s41586-019-1822-y

Isard, S. A. (1986). Factors influencing soil moisture and plant community distribution on Niwot Ridge, Front Range, Colorado, U.S.A. *Arctic and Alpine Research*, *18*(1), 83–96. https://doi.org/10.1080/00040851.1986.12004065

Iversen, C. M., Sloan, V. L., Sullivan, P. F., Euskirchen, E. S., McGuire, A. D., Norby, R. J., et al. (2015). The unseen iceberg: plant roots in arctic tundra. *New Phytologist*, *205*(1), 34–58. https://doi.org/10.1111/nph.13003

Jackson, R. B., Canadell, J., Ehleringer, J. R., Mooney, H. A., Sala, O. E., & Schulze, E. D. (1996). A global analysis of root distributions for terrestrial biomes. *Oecologia*, *108*(3), 389–411. https://doi.org/10.1007/BF00333714

Keenan, T. F., Hollinger, D. Y., Bohrer, G., Dragoni, D., Munger, J. W., Schmid, H. P., & Richardson, A. D. (2013). Increase in forest water-use efficiency as atmospheric carbon dioxide concentrations rise. *Nature*, *499*(7458), 324–327. https://doi.org/10.1038/nature12291

Kennedy, D., Swenson, S., Oleson, K. W., Lawrence, D. M., Fisher, R., Lola da Costa, A. C., & Gentine, P. (2019). Implementing plant hydraulics in the Community Land Model, version 5. *Journal of Advances in Modeling Earth Systems*, *11*(2), 485–513. https://doi.org/10.1029/2018MS001500

Kittel, T. G. F., Williams, M. W., Chowanski, K., Hartman, M., Ackerman, T., Losleben, M., & Blanken, P. D. (2015). Contrasting long-term alpine and subalpine precipitation trends in

a mid-latitude North American mountain system, Colorado Front Range, USA. *Plant Ecology & Diversity*, *8*(5–6), 607–624. https://doi.org/10.1080/17550874.2016.1143536

Knowles, J. F. (2022a). *AmeriFlux BASE US-NR3 Niwot Ridge Alpine (T-Van West), Ver. 3-5, AmeriFlux AMP, (Dataset)*. Retrieved from https://doi.org/10.17190/AMF/1804491

Knowles, J. F. (2022b). *AmeriFlux BASE US-NR4 Niwot Ridge Alpine (T-Van East), Ver. 3-5, AmeriFlux AMP, (Dataset)*. Retrieved from https://doi.org/10.17190/AMF/1804492

Knowles, J. F., Blanken, P. D., Williams, M. W., & Chowanski, K. M. (2012). Energy and surface moisture seasonally limit evaporation and sublimation from snow-free alpine tundra. *Agricultural and Forest Meteorology*, *157*, 106–115. https://doi.org/10.1016/j.agrformet.2012.01.017

Knowles, J. F., Harpold, A. A., Cowie, R., Zeliff, M., Barnard, H. R., Burns, S. P., et al. (2015). The relative contributions of alpine and subalpine ecosystems to the water balance of a mountainous, headwater catchment. *Hydrological Processes*, *29*(22), 4794–4808. https://doi.org/10.1002/hyp.10526

Knowles, J. F., Blanken, P. D., & Williams, M. W. (2016). Wet meadow ecosystems contribute the majority of overwinter soil respiration from snow-scoured alpine tundra. *Journal of Geophysical Research: Biogeosciences*, *121*(4), 1118–1130. https://doi.org/10.1002/2015JG003081

Knowles, J. F., Blanken, P. D., Lawrence, C. R., & Williams, M. W. (2019). Evidence for non-steady-state carbon emissions from snow-scoured alpine tundra. *Nature Communications*, *10*(1), 1306. https://doi.org/10.1038/s41467-019-09149-2

Körner, C., & Hiltbrunner, E. (2021). Why Is the Alpine Flora Comparatively Robust against Climatic Warming? *Diversity*, *13*(8), 383. https://doi.org/10.3390/d13080383

Koven, C. D., Riley, W. J., Subin, Z. M., Tang, J. Y., Torn, M. S., Collins, W. D., et al. (2013). The effect of vertically resolved soil biogeochemistry and alternate soil C and N models on C dynamics of CLM4. *Biogeosciences*, *10*(11), 7109–7131. https://doi.org/10.5194/bg-10-7109-2013

Lawrence, D. M., Fisher, R. A., Koven, C. D., Oleson, K. W., Swenson, S. C., Bonan, G., et al. (2019). The Community Land Model Version 5: Description of new features, benchmarking, and impact of forcing uncertainty. *Journal of Advances in Modeling Earth Systems*, *11*(12), 4245–4287. https://doi.org/10.1029/2018MS001583

Lenoir, J., Graae, B. J., Aarrestad, P. A., Alsos, I. G., Armbruster, W. S., Austrheim, G., et al. (2013). Local temperatures inferred from plant communities suggest strong spatial buffering of climate warming across Northern Europe. *Global Change Biology*, *19*(5), 1470–1481. https://doi.org/10.1111/gcb.12129

Lenoir, J., Hattab, T., & Pierre, G. (2017). Climatic microrefugia under anthropogenic climate change: implications for species redistribution. *Ecography*, *40*(2), 253–266. https://doi.org/10.1111/ecog.02788

Lipson, D. A., Schmidt, S. K., & Monson, R. K. (1999). Links between microbial population dynamics and Nitrogen availability in an alpine ecosystem. *Ecology*, *80*(5), 1623–1631. https://doi.org/10.1890/0012-9658(1999)080[1623:LBMPDA]2.0.CO;2

Lipson, D. A., Schmidt, S. K., & Monson, R. K. (2000). Carbon availability and temperature control the post-snowmelt decline in alpine soil microbial biomass. *Soil Biology and Biochemistry*, *32*(4), 441–448. https://doi.org/10.1016/S0038-0717(99)00068-1

Litaor, M. I., Williams, M., & Seastedt, T. R. (2008). Topographic controls on snow distribution, soil moisture, and species diversity of herbaceous alpine vegetation, Niwot Ridge,

Colorado. *Journal of Geophysical Research: Biogeosciences*, *113*(G2). https://doi.org/10.1029/2007JG000419

Loescher, H., Ayres, E., Duffy, P., Luo, H., & Brunke, M. (2014). Spatial variation in soil properties among North American ecosystems and guidelines for sampling designs. *PLOS ONE*, *9*(1), e83216. https://doi.org/10.1371/journal.pone.0083216

Lombardozzi, D. L., Wieder, W. R., Sobhani, N., Bonan, G. B., Durden, D., Lenz, D., et al. (2023). *Overcoming barriers to enable convergence research by integrating ecological and climate sciences: The NCAR-NEON system Version 1* (preprint). Earth and space science informatics. https://doi.org/10.5194/egusphere-2023-271

Luo, J., Huang, A., Lyu, S., Lin, Z., Gu, C., Li, Z., et al. (2023). Improved Performance of CLM5.0 Model in Frozen Soil Simulation Over Tibetan Plateau by Implementing the Vegetation Emissivity and Gravel Hydrothermal Schemes. *Journal of Geophysical Research: Atmospheres*, *128*(6), e2022JD038021. https://doi.org/10.1029/2022JD038021

Mao, J., Ricciuto, D. M., Thornton, P. E., Warren, J. M., King, A. W., Shi, X., et al. (2016). Evaluating the Community Land Model in a pine stand with shading manipulations and $^{13}CO_2$ labeling. *Biogeosciences*, *13*(3), 641–657. https://doi.org/10.5194/bg-13-641-2016

May, D. E., Webber, P. J., & May, T. A. (1982). Success of Transplanted Alpine Tundra Plants on Niwot Ridge, Colorado. *Journal of Applied Ecology*, *19*(3), 965–976.

McGuire, C. R., Nufio, C. R., Bowers, M. D., & Guralnick, R. P. (2012). Elevation-dependent temperature trends in the Rocky Mountain Front Range: Changes over a 56- and 20-year record. *PLOS ONE*, *7*(9), e44370. https://doi.org/10.1371/journal.pone.0044370

McLaughlin, B. C., Ackerly, D. D., Klos, P. Z., Natali, J., Dawson, T. E., & Thompson, S. E. (2017). Hydrologic refugia, plants, and climate change. *Global Change Biology*, *23*(8), 2941–2961. https://doi.org/10.1111/gcb.13629

Mekonnen, Z. A., Riley, W. J., Berner, L. T., Bouskill, N. J., Torn, M. S., Iwahana, G., et al. (2021). Arctic tundra shrubification: a review of mechanisms and impacts on ecosystem carbon balance. *Environmental Research Letters*, *16*(5), 053001. https://doi.org/10.1088/1748-9326/abf28b

Morse, J. F., & Niwot Ridge LTER. (2022). *Climate data for saddle catchment sensor network, 2017 - ongoing. ver 4*. Environmental Data Initiative. Retrieved from https://doi.org/10.6073/pasta/598894834ea3bae61d7550c30da06565

Mote, P. W., Hamlet, A. F., Clark, M. P., & Lettenmaier, D. P. (2005). Declining mountain snowpack in western North America. *Bulletin of the American Meteorological Society*, *86*(1), 39–50. https://doi.org/10.1175/BAMS-86-1-39

Mountain Research Initiative EDW Working Group. (2015). Elevation-dependent warming in mountain regions of the world. *Nature Climate Change*, *5*(5), 424–430. https://doi.org/10.1038/nclimate2563

Musselman, K. N., Clark, M. P., Liu, C., Ikeda, K., & Rasmussen, R. (2017). Slower snowmelt in a warmer world. *Nature Climate Change*, *7*(3), 214–219. https://doi.org/10.1038/nclimate3225

Musselman, K. N., Addor, N., Vano, J. A., & Molotch, N. P. (2021). Winter melt trends portend widespread declines in snow water resources. *Nature Climate Change*, *11*, 418–424. https://doi.org/10.1038/s41558-021-01014-9

Oldfather, M. F., & Ackerly, D. D. (2019). Microclimate and demography interact to shape stable population dynamics across the range of an alpine plant. *New Phytologist*, *222*(1), 193–205. https://doi.org/10.1111/nph.15565

Opedal, Ø. H., Armbruster, W. S., & Graae, B. J. (2015). Linking small-scale topography with microclimate, plant species diversity and intra-specific trait variation in an alpine landscape. *Plant Ecology & Diversity*, *8*(3), 305–315. https://doi.org/10.1080/17550874.2014.987330

Panetta, A. M., Stanton, M. L., & Harte, J. (2018). Climate warming drives local extinction: Evidence from observation and experimentation. *Science Advances*, *4*(2), eaaq1819. https://doi.org/10.1126/sciadv.aaq1819

Pascale, S., Boos, W. R., Bordoni, S., Delworth, T. L., Kapnick, S. B., Murakami, H., et al. (2017). Weakening of the North American monsoon with global warming. *Nature Climate Change*, *7*(11), 806–812. https://doi.org/10.1038/nclimate3412

Schadt, C. W., Martin, A. P., Lipson, D. A., & Schmidt, S. K. (2003). Seasonal dynamics of previously unknown fungal lineages in tundra soils. *Science*, *301*(5638), 1359–1361. https://doi.org/10.1126/science.1086940

Scherrer, D., & Körner, C. (2011). Topographically controlled thermal-habitat differentiation buffers alpine plant diversity against climate warming. *Journal of Biogeography*, *38*(2), 406–416. https://doi.org/10.1111/j.1365-2699.2010.02407.x

Schmidt, S. K., King, A. J., Meier, C. L., Bowman, W. D., Farrer, E. C., Suding, K. N., & Nemergut, D. R. (2015). Plant–microbe interactions at multiple scales across a high-elevation landscape. *Plant Ecology & Diversity*, *8*(5–6), 703–712. https://doi.org/10.1080/17550874.2014.917737

Schuur, E. A. G., McGuire, A. D., Schädel, C., Grosse, G., Harden, J. W., Hayes, D. J., et al. (2015). Climate change and the permafrost carbon feedback. *Nature*, *520*(7546), 171–179. https://doi.org/10.1038/nature14338

Seddon, A. W. R., Macias-Fauria, M., Long, P. R., Benz, D., & Willis, K. J. (2016). Sensitivity of global terrestrial ecosystems to climate variability. *Nature*, *531*(7593), 229–232. https://doi.org/10.1038/nature16986

Spasojevic, M. J., & Suding, K. N. (2012). Inferring community assembly mechanisms from functional diversity patterns: the importance of multiple assembly processes. *Journal of Ecology*, *100*(3), 652–661. https://doi.org/10.1111/j.1365-2745.2011.01945.x

Spasojevic, M. J., Bowman, W. D., Humphries, H. C., Seastedt, T. R., & Suding, K. N. (2013). Changes in alpine vegetation over 21 years: Are patterns across a heterogeneous landscape consistent with predictions? *Ecosphere*, *4*(9), art117. https://doi.org/10.1890/ES13-00133.1

Spasojevic, M. J., Harrison, S., Day, H. W., & Southard, R. J. (2014). Above- and belowground biotic interactions facilitate relocation of plants into cooler environments. *Ecology Letters*, *17*(6), 700–709. https://doi.org/10.1111/ele.12272

Steinbauer, M. J., Grytnes, J.-A., Jurasinski, G., Kulonen, A., Lenoir, J., Pauli, H., et al. (2018). Accelerated increase in plant species richness on mountain summits is linked to warming. *Nature*, *556*(7700), 231–234. https://doi.org/10.1038/s41586-018-0005-6

Sturm, M., Racine, C., & Tape, K. (2001). Increasing shrub abundance in the Arctic. *Nature*, *411*(6837), 546–547. https://doi.org/10.1038/35079180

Sulman, B. N., Salmon, V. G., Iversen, C. M., Breen, A. L., Yuan, F., & Thornton, P. E. (2021). Integrating Arctic Plant Functional Types in a Land Surface Model Using Above- and

Belowground Field Observations. *Journal of Advances in Modeling Earth Systems*, *13*(4), e2020MS002396. https://doi.org/10.1029/2020MS002396

Swenson, S. C., & Lawrence, D. M. (2014). Assessing a dry surface layer-based soil resistance parameterization for the Community Land Model using GRACE and FLUXNET-MTE data. *Journal of Geophysical Research: Atmospheres*, *119*(17), 10,299-10,312. https://doi.org/10.1002/2014JD022314

Swenson, Sean C., Clark, M., Fan, Y., Lawrence, D. M., & Perket, J. (2019). Representing intrahillslope lateral subsurface flow in the Community Land Model. *Journal of Advances in Modeling Earth Systems*, *11*(12), 4044–4065. https://doi.org/10.1029/2019MS001833

Taylor, R. V., & Seastedt, T. R. (1994). Short- and long-term patterns of soil moisture in alpine tundra. *Arctic and Alpine Research*, *26*(1), 14–20. https://doi.org/10.2307/1551871

Walker, D., Morse, J., & Niwot Ridge LTER. (2022). *Snow depth data for saddle snowfence, 1992 - ongoing. ver 13.* Environmental Data Initiative. Retrieved from https://doi.org/10.6073/pasta/a6a30132f9d4e2d9a0763e7a7faef619

Walker, M., Smith, J., Humphries, H., & Niwot Ridge LTER. (2022). *Aboveground net primary productivity data for Saddle grid, 1992 - ongoing. ver 6*. Environmental Data Initiative. Retrieved from https://doi.org/10.6073/pasta/b0cdc0cf7c4442f1b2ffc569e9890968

Walker, M. D., Webber, P. J., Arnold, E. H., & Ebert-May, D. (1994). Effects of interannual climate variation on aboveground phytomass in alpine vegetation. *Ecology*, *75*(2), 393–408. https://doi.org/10.2307/1939543

Walker, M. D., Wahren, C. H., Hollister, R. D., Henry, G. H. R., Ahlquist, L. E., Alatalo, J. M., et al. (2006). Plant community responses to experimental warming across the tundra

biome. *Proceedings of the National Academy of Sciences*, *103*(5), 1342–1346. https://doi.org/10.1073/pnas.0503198103

Wang, Q., Fan, X., & Wang, M. (2016). Evidence of high-elevation amplification versus Arctic amplification. *Scientific Reports*, *6*(1), 19219. https://doi.org/10.1038/srep19219

Wentz, K. F., Neff, J. C., & Suding, K. N. (2019). Leaf temperatures mediate alpine plant communities' response to a simulated extended summer. *Ecology and Evolution*, *9*(3), 1227–1243. https://doi.org/10.1002/ece3.4816

Wieder, W. R., Knowles, J. F., Blanken, P. D., Swenson, S. C., & Suding, K. N. (2017). Ecosystem function in complex mountain terrain: Combining models and long-term observations to advance process-based understanding. *Journal of Geophysical Research: Biogeosciences*, *122*(4), 825–845. https://doi.org/10.1002/2016JG003704

Wieder, W. R., Kennedy, D., Lehner, F., Musselman, K. N., Rodgers, K. B., Rosenbloom, N., et al. (2022). Pervasive alterations to snow-dominated ecosystem functions under climate change. *Proceedings of the National Academy of Sciences*, *119*(30), e2202393119. https://doi.org/10.1073/pnas.2202393119

Wigmore, O., & Niwot Ridge LTER. (2021). *5cm multispectral imagery from UAV campaign at Niwot Ridge, 2017 ver. 1*. Environmental Data Initiative. Retrieved from https://doi.org/10.6073/pasta/a4f57c82ad274aa2640e0a79649290ca

Williams, M. W., Bardsley, T., & Rikkers, M. (1998). Overestimation of snow depth and inorganic nitrogen wetfall using NADP data, Niwot Ridge, Colorado. *Atmospheric Environment*, *32*(22), 3827–3833. https://doi.org/10.1016/S1352-2310(98)00009-0

Winkler, D. E., Butz, R. J., Germino, M. J., Reinhardt, K., & Kueppers, L. M. (2018). Snowmelt Timing Regulates Community Composition, Phenology, and Physiological Performance

of Alpine Plants. *Frontiers in Plant Science*, *9*. Retrieved from https://www.frontiersin.org/articles/10.3389/fpls.2018.01140

Wookey, P. A., Aerts, R., Bardgett, R. D., Baptist, F., Bråthen, K. A., Cornelissen, J. H. C., et al. (2009). Ecosystem feedbacks and cascade processes: understanding their role in the responses of Arctic and alpine ecosystems to environmental change. *Global Change Biology*, *15*(5), 1153–1172. https://doi.org/10.1111/j.1365-2486.2008.01801.x

Wutzler, T., Lucas-Moffat, A., Migliavacca, M., Knauer, J., Sickel, K., Šigut, L., et al. (2018). Basic and extensible post-processing of eddy covariance flux data with REddyProc. *Biogeosciences*, *15*(16), 5015–5030. https://doi.org/10.5194/bg-15-5015-2018

Yang, Y., Klein, J. A., Winkler, D. E., Peng, A., Lazarus, B. E., Germino, M. J., et al. (2020). Warming of alpine tundra enhances belowground production and shifts community towards resource acquisition traits. *Ecosphere*, *11*(10), e03270. https://doi.org/10.1002/ecs2.3270

Zellweger, F., De Frenne, P., Lenoir, J., Vangansbeke, P., Verheyen, K., Bernhardt-Römermann, M., et al. (2020). Forest microclimate dynamics drive plant responses to warming. *Science*, *368*(6492), 772–775. https://doi.org/10.1126/science.aba6880

Journal of Geophysical Research: Biogeosciences

Supporting Information for

Topographic heterogeneity and aspect moderate exposure to climate change across an alpine tundra hillslope

K. R. Jay[1], W. R. Wieder[1,2], S. C. Swenson[2], J. F. Knowles[3], S. Elmendorf[1,4], H. Holland-Moritz[5], K. N. Suding[1,4]

[1]Institute of Arctic and Alpine Research, University of Colorado, 4001 Discovery Dr, Boulder, CO 80303, USA.

[2]National Center for Atmospheric Research, 1850 Table Mesa Dr, Boulder, CO 80305, USA

[3]Department of Earth and Environmental Sciences, California State University, 400 W. First St, Chico, CA 95929, USA.

[4]Department of Ecology and Evolutionary Biology, University of Colorado, 1900 Pleasant St, Boulder, CO 80302, USA.

[5]Department of Natural Resources and the Environment, University of New Hampshire, 114 James Hall, 56 College Rd, Durham, NH 03824, USA.

Contents of this file

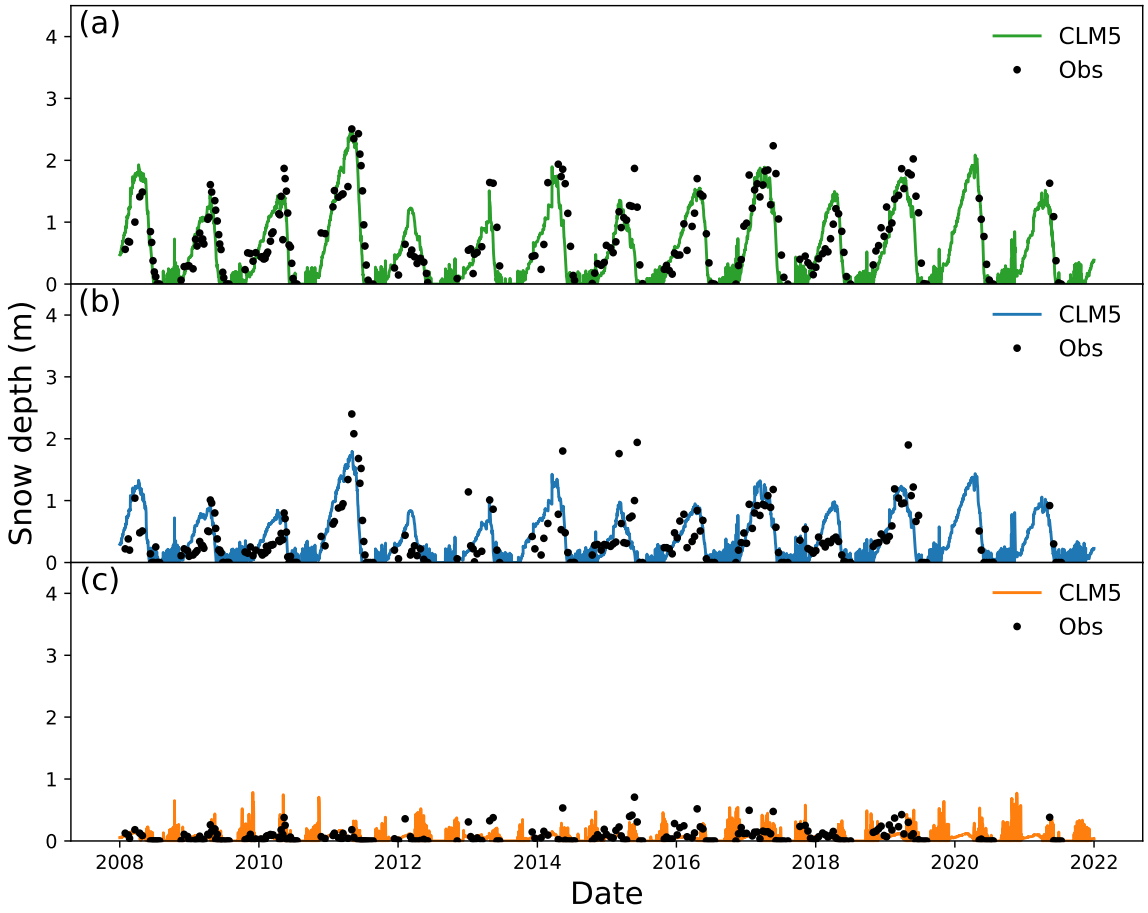

Figure S1. CLM simulations capture the observed variability in the magnitude and timing of snow depth across all three vegetation communities at Niwot Ridge. Time series of observations and CLM simulations from 2008-2021 configured for (a) moist, (b) wet, and (c) dry meadows. Colored lines denote CLM simulations and black points denote ~biweekly snow depth measurements from the Saddle at Niwot Ridge, CO that were averaged by vegetation community and date.

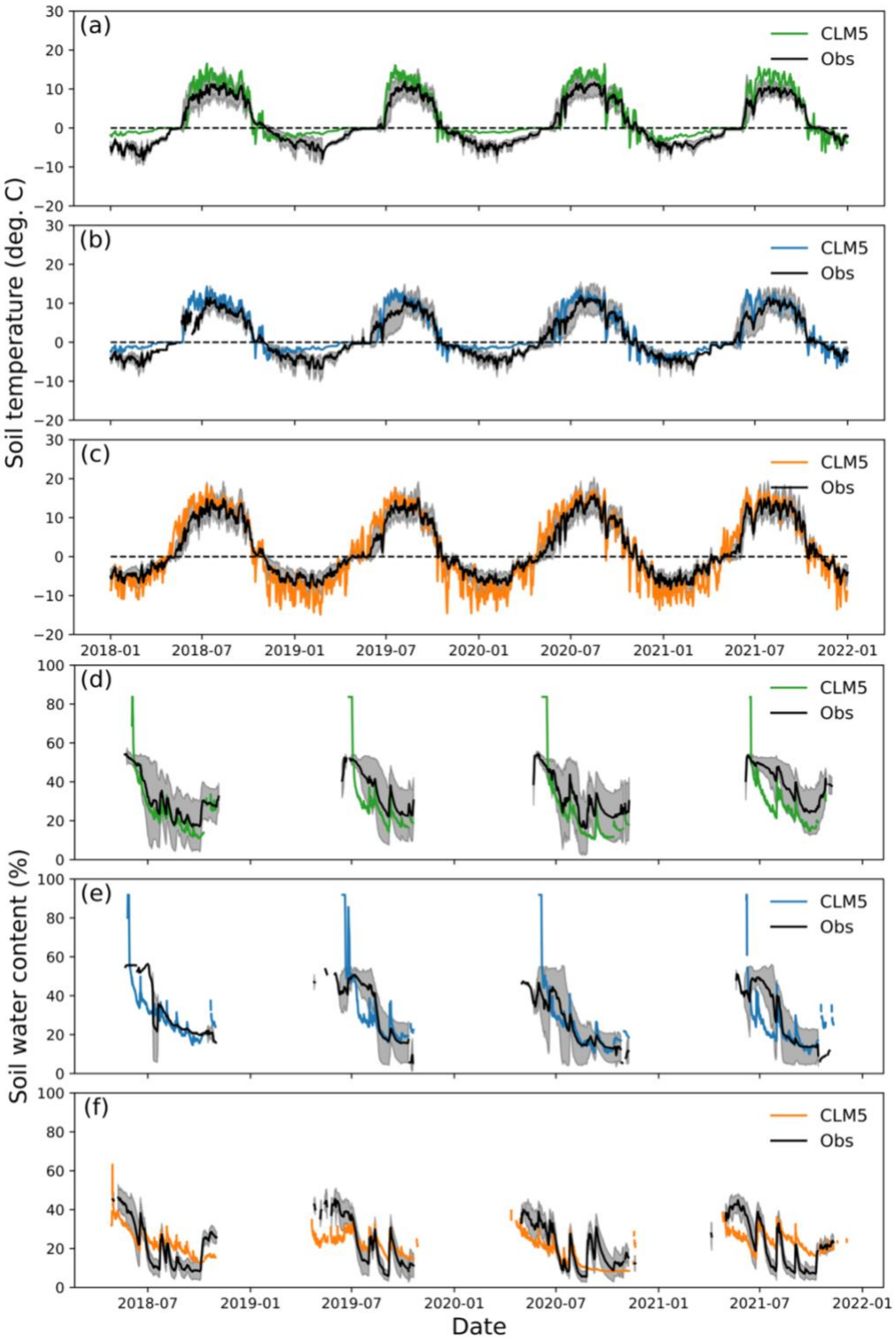

Figure S2. Time series of observations (mean ± SD) and CLM simulations configured for moist, wet, and dry meadows. (a-c) volumetric soil moisture, and (d-f) soil temperature from 2018-2022 at 5 cm (observations) and 4 cm (CLM simulations) depths. Colored lines denote CLM simulations and black lines denote observations from the sensor network array at Niwot Ridge, CO, where values were averaged across plots for each vegetation community.

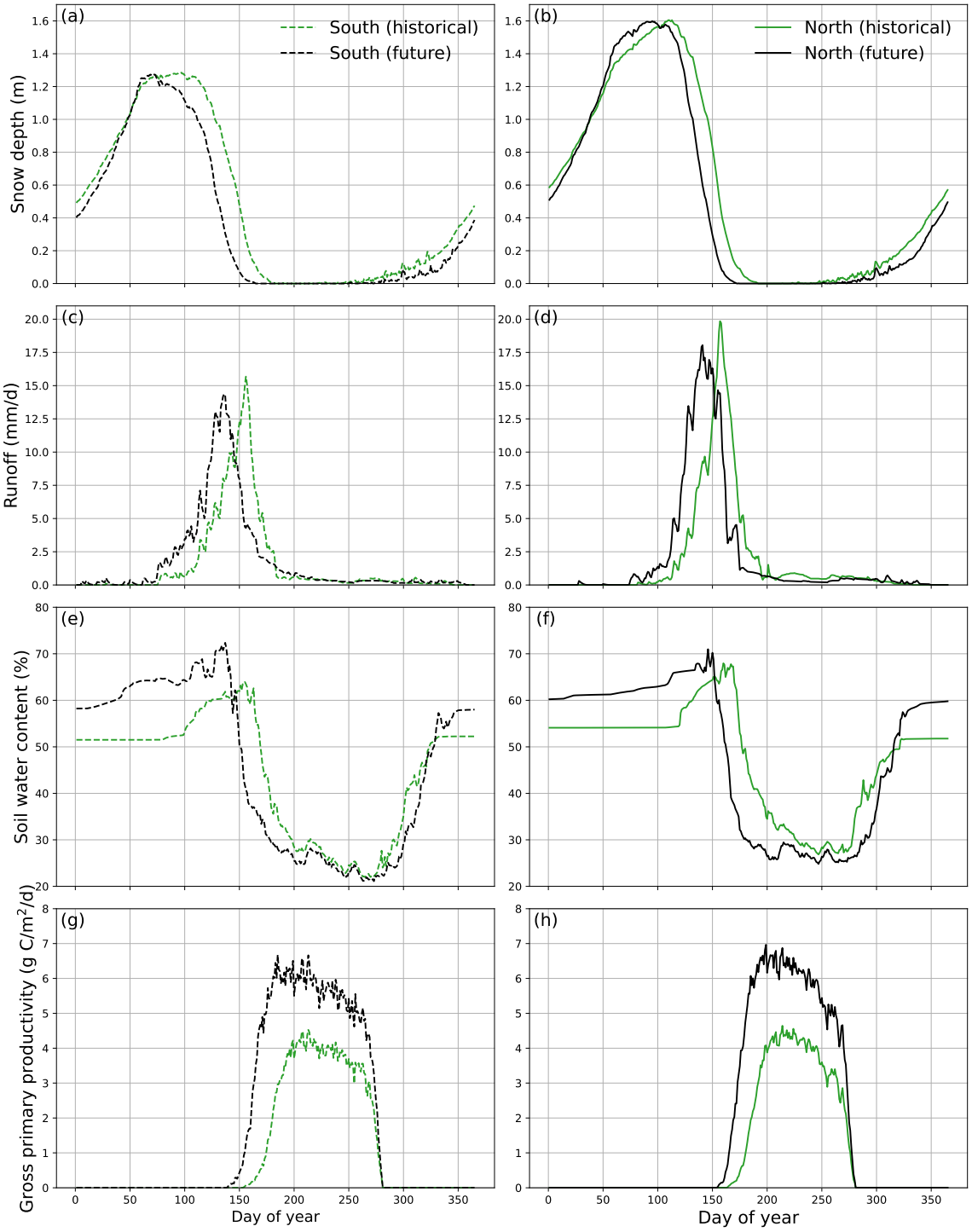

Figure S3. Mean annual climatology of (a, b) snow depth (m), (c, d) runoff (mm/d), (e, f) soil moisture (%), and (g, h) productivity in the moist meadow (upland) column for historical (green lines; 2008-2021) and future (black lines; 2086-2099) time periods. Results from south aspect (dashed lines) are shown in left column and those from north aspect (solid lines) are in right column. Values were averaged by day of year for each time period and aspect. Negative runoff values occur when inflow from uphill is greater than outflow.

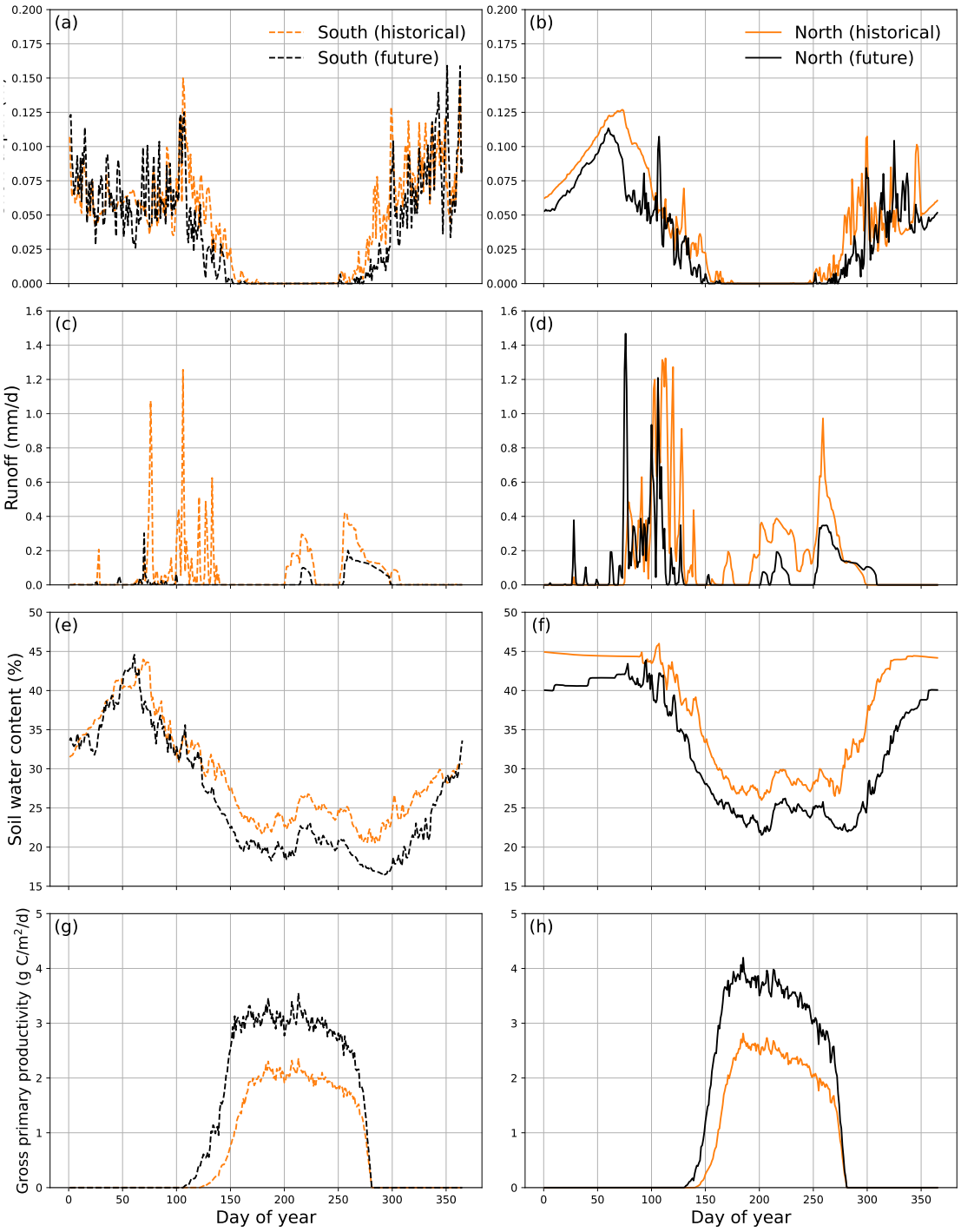

Figure S4. Mean annual climatology of (a, b) snow depth (m), (c, d) runoff (mm/d), (e, f) soil moisture (%), and (g, h) productivity in the dry meadow (upland) column for historical (orange lines; 2008-2021) and future (black lines; 2086-2099) time periods. Results from south aspect (dashed lines) are shown in left column and those from north aspect (solid lines) are in right column. Values were averaged by day of year for each time period and aspect. Negative runoff values occur when inflow from uphill is greater than outflow.

Parameter	Description	Units	Moist Meadow	Wet Meadow	Dry Meadow	Default
slatop[1]	specific leaf area	m^2/gC	0.0215	0.029	0.015	0.0402
leafcn[1]	leaf C:N	gC/gN	19.6	17.7	18.5	28.03
ndays_on[2]	# days to complete leaf onset	days	21	28	25	10
crit_onset_gdd_sf[2]	scale factor modifying GDD	unitless	1	1	1.7	1
kmax	plant maximum conductance	mm H_2O/mm H_2O/sec	2.42E-09	2.42E-09	2.30E-10	2.42E-09
krmax	root maximum conductance	mm H_2O/mm H_2O/sec	8.05E-11	8.05E-11	2.05E-11	8.05E-11
$jmaxb_0$	baseline proportion of N for electron transport	unitless	0.0225	0.0225	0.0225	0.0331
$jmaxb_1$	response of electron transport rate to light availability	unitless	0.1	0.1	0.1	0.1745
froot_leaf	new fine root C per new leaf C allocation	gC/gC	1.5	1.5	2	2
d_max	dry surface layer thickness	mm	10	10	10	15
h_bedrock	depth to bedrock	m	1.3	1	1	
wat_sat	water saturation (porosity)	m^3/m^3			wat_sat/2	
organic[3]	organic matter density	kg/ m^3	80.7	107.6	80.7	
sand[3]	percent sand	%	49.3	44.4	49.3	
clay[3]	percent clay	%	12.7	14	12.7	

[1]Values for each vegetation community from Spasojevic et al., (2013).
[2]Values for each vegetation community derived from Niwot Ridge phenocam green chromatic coordinate (GCC) data set (Elwood et al., 2022) and resulting phenometric calculations (unpublished data)
[3]Values based on National Ecological Observatory Network (NEON) Megapit (Lombardozzi et al. 2013)

Table S1. Modifications to foliar, hydraulic, and photosynthetic parameters and soil properties to better represent moist, wet, and dry alpine meadow environments. Default values specified in the parameter file are listed for comparison where available. GDD stands for growing degree days.